RESEARCH ARTICLE

Key Points:
- The Fenghuoshan Group was deposited from late Cretaceous to early Eocene time
- The Fenghuoshan Group was likely sourced from the central Qiangtang Terrane
- Crustal shortening of the Hoh Xil Basin occurred from Eocene to Oligocene time

Supporting Information:
- Readme
- Table S1
- Table S2
- Table S3
- Table S4
- Table S5
- Table S6
- Table S7
- Table S8
- Figure S1
- Figure S2
- Figure S3
- Figure S4
- Figure S5
- Figure S6
- Figure S7

Correspondence to:
L. M. Staisch,
staischl@umich.edu

A Cretaceous-Eocene depositional age for the Fenghuoshan Group, Hoh Xil Basin: Implications for the tectonic evolution of the northern Tibet Plateau

Lydia M. Staisch[1], Nathan A. Niemi[1], Chang Hong[2], Marin K. Clark[1], David B. Rowley[3], and Brian Currie[4]

[1]Department of Earth and Environmental Sciences, University of Michigan, Ann Arbor, Michigan, USA, [2]Institute of Earth Environment, CAS, Xi'an, China, [3]Department of the Geophysical Sciences, University of Chicago, Chicago, Illinois, USA, [4]Department of Geology and Environmental Earth Science, Miami University, Oxford, Ohio, USA

Abstract The Fenghuoshan Group marks the initiation of terrestrial deposition in the Hoh Xil Basin and preserves the first evidence of uplift above sea level of northern Tibet. The depositional age of the Fenghuoshan Group is debated as are the stratigraphic relationships between the Fenghuoshan Group and other terrestrial sedimentary units in the Hoh Xil Basin. We present new radiometric dates and a compilation of published biostratigraphic data which are used to reinterpret existing magnetostratigraphic data from the Fenghuoshan Group. From these data, we infer an 85–51 Ma depositional age range for the Fenghuoshan Group. U-Pb detrital zircon age spectra from this unit are compared to age spectra from Tibetan terranes and Mesozoic sedimentary sequences to determine a possible source terrane for Fenghuoshan Group strata. We propose that these strata were sourced from the Qiangtang Terrane and may share a common sediment source with Cretaceous sedimentary rocks in Nima Basin. Field relationships and compiled biostratigraphic data indicate that the Fenghuoshan and Tuotuohe Groups are temporally distinct units. We report late Oligocene ages for undeformed basalt flows that cap tilted Fenghuoshan Group strata. Together, our age constraints and field relationships imply exhumation of the central Qiangtang Terrane from the Late Cretaceous to earliest Eocene, followed by Eocene-Oligocene deformation, and shortening of the northern Qiangtang and southern Songpan-Ganzi terranes. Crustal shortening within the Hoh Xil Basin ceased by late Oligocene time as is evident from flat-lying basaltic rocks, which cap older, deformed strata.

1. Introduction

For decades, the Tibetan Plateau has been studied as an example of Cenozoic continental collision and associated crustal thickening and topographic growth. Numerical and conceptual models have generally considered the Indo-Asian collision to be a single, ongoing tectonic event that has led to the growth of the Tibetan Plateau. Such models have invoked a variety of mechanisms to build Tibet, including continental underplating of India [*Argand*, 1924; *Powell*, 1986; *Zhao and Morgan*, 1987], distributed shortening and thickening of the Eurasian lithosphere [*England and McKenzie*, 1982; *Dewey et al.*, 1988; *England and Houseman*, 1986], progressive stepwise uplift along discrete lithospheric blocks [*Tapponnier et al.*, 2001], or removal of the mantle lithosphere followed by replacement with hot, buoyant asthenosphere [*Molnar et al.*, 1993]. The southern margin of Eurasia, however, has been the site of active subduction and continental accretion since the early Mesozoic [*Dewey et al.*, 1988; *Şengör and Natal'in*, 1996; *Yin and Harrison*, 2000], and the transition from oceanic subduction to continental collision in any such Alpine-style orogeny may include events such as accretion of small island arcs or continental fragments, rifting and closure of interarc basins, and orogenesis during the subduction phase. These processes affect the rheology and elevation of the continental margin prior to continental collision [*Cloos*, 1993; *Boutelier et al.*, 2003] and may give rise to a unique deformation pattern within the orogen itself [*Royden and Burchfiel*, 1989; *Dilek*, 2006].

It has been proposed that much of the ~2500–3000 km convergence of India with Eurasia since the widely accepted ~50 Ma age of Indo-Asian collision [*Rowley*, 1996; *Molnar and Stock*, 2009; *Dupont-Nivet et al.*, 2010; *Najman et al.*, 2010] was accommodated via crustal shortening [*Dewey et al.*, 1988; *England and Houseman*, 1986; *Dupont-Nivet et al.*, 2004; *Najman et al.*, 2010]. However, the amount of crustal shortening required to accommodate postcollisional Indo-Asian convergence is difficult to reconcile, particularly since there is

relatively little evidence for large-scale crustal shortening in the Lhasa and southern Qiangtang terranes since 50 Ma [*Burg et al.*, 1983; *England and Searle*, 1986; *Murphy et al.*, 1997; *Kapp et al.*, 2005, 2007a, 2007b; *DeCelles et al.*, 2007a; *Hetzel et al.*, 2011; *Rohrmann et al.*, 2012]. The formation of a thick continental margin by the Late Cretaceous may have preconditioned the Asian lithosphere's response to further deformation, such that high gravitational potential energy in southern Tibet would inhibit further thickening and elevation gain [*England and Searle*, 1986; *Kong et al.*, 1997]. Instead, a precollisional thick continental margin may favor syncollisional and postcollisional crustal thickening in regions to the north, more distal to the plate boundary and may explain limited surface deformation observed within the Lhasa and southern Qiangtang terranes during the early to midstages of continental collision.

The Hoh Xil Basin, located in north central Tibet, contains a generally complete stratigraphic sequence that ranges from Late Cretaceous to Miocene in age. This locale potentially records the far-field lithospheric response of the transition from subduction to collision at the Indo-Asian plate boundary. Tectonic interpretation of geologic and geochemical data derived from sedimentary strata within the Hoh Xil Basin relies heavily on the depositional age of these strata. However, the timing of deposition in the Hoh Xil Basin, as well as the division of lithostratigraphic units, their depositional relationships, and stratigraphic nomenclature are subject to debate [*Yin et al.*, 1988; *Zhong*, 1989; *Li and Yuan*, 1990; *Ji*, 1994; *Liu et al.*, 2001, 2003; *An et al.*, 2004; *Yi et al.*, 2004; *Li et al.*, 2012]. In this study, we redefine the depositional age of nonmarine strata in the Hoh Xil Basin based on new radiometric ages from volcanic units and reinterpretation of biostratigraphic and magnetostratigraphic records. Based on our revised depositional ages for nonmarine strata and field observations, we reevaluate the stratigraphy of the Hoh Xil Basin and its significance for understanding the tectonic evolution of the Tibetan Plateau.

2. Geologic Setting

The Fenghuoshan Group (风火山群) is a sedimentary sequence that was deposited within the Hoh Xil Basin, an 83,000 km^2 region in the north central Tibetan Plateau that extends from the Tanggula Shan northward to the Kunlun Shan (Figure 1). The sedimentary sequence overlies and obscures the Jinsha Suture; thus, the Fenghuoshan Group was deposited within the northernmost Qiangtang and southernmost Songpan-Ganzi terranes. The main subbasin in which the Fenghuoshan Group was deposited is located near the town of Erdaguo, in what is now the Fenghuoshan Range (Figure 1). The Fenghuoshan Range extends roughly 35 km north to south and reaches elevations of ~5300 m. Postdepositional deformation of the Fenghuoshan Range has resulted in the exposure of ~5.8 km of the Fenghuoshan Group [*Zhong*, 1989] in the hanging wall of a regionally extensive thrust fault (Figure 1), one of the most stratigraphically extensive sections known for this sedimentary unit.

The Fenghuoshan Group is terrestrial in origin and is largely composed of mudstone, siltstone, sandstone, and conglomerate as well as subordinate limestone and evaporite layers [*Leeder et al.*, 1988; *Zhong*, 1989; *Ji*, 1994; *Liu et al.*, 2001; *An et al.*, 2004]. These strata were deposited unconformably over the Triassic Jieza (结扎群), Triassic Batang (巴颜喀拉山群), and Jurassic Yanshiping (雁石坪群) Groups [*Kidd et al.*, 1988; *Qinghai Bureau of Geology and Mineral Resources* (QBGMR), 1989a, 1989b; *An et al.*, 2004]. The depositional environment of the Fenghuoshan Group is predominantly fluvial and fan delta, with a minor distal lacustrine component [*Leeder et al.*, 1988; *Liu and Wang*, 2001a; *Liu et al.*, 2001]. Paleocurrent directions suggest that the Fenghuoshan Group was sourced predominantly from the south [*Leeder et al.*, 1988; *Liu and Wang*, 2001b; *Liu et al.*, 2001; *Yi et al.*, 2008; *Li et al.*, 2012]. The sedimentary rocks of the Fenghuoshan Group are characteristically deep brick red to purple in color, with occasional copper-bearing green sandstone [*Yin et al.*, 1988; *Li et al.*, 2005], indicating considerable oxidation. Fossils present in the Fenghuoshan Group include ostracods, gastropods, charophytes, pollen, and plant material [*Leeder et al.*, 1988; *Yin et al.*, 1988; *QBGMR*, 1989a, 1989b; *Zhong*, 1989; *Li and Yuan*, 1990; *Liu et al.*, 2001; *An et al.*, 2004; *Cyr et al.*, 2005].

Overlying the Fenghuoshan Group are the fluvial and lacustrine Tuotuohe (沱沱河群) and Yaxicuo (雅西措群; also published as the Chabaoma) Groups [*Yin et al.*, 1988; *QBGMR*, 1989a, 1989b; *An et al.*, 2004]. These strata exhibit relatively moderate syndepositional to postdepositional deformation. The Miocene Wudaoliang Group, which is composed of lacustrine carbonate and unconformably overlies the Yaxicuo Group, exhibits only mild deformation [*Liu and Wang*, 2001a; *Liu et al.*, 2001, 2003; *Z. Duan et al.*, 2007; *Li*
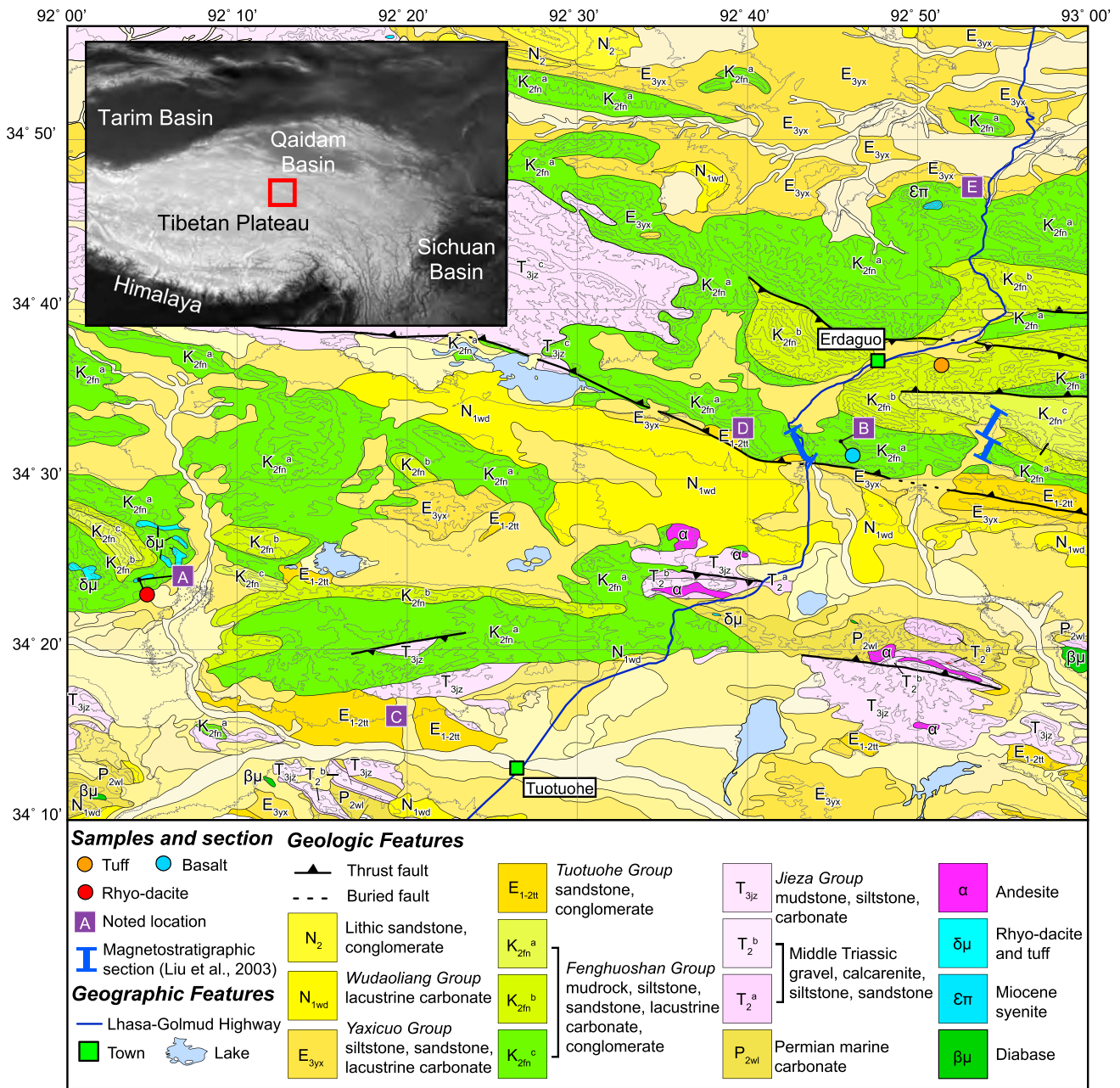
Figure 1. Geologic map of the area around the Fenghuoshan Range, Hoh Xil Basin (modified from *Qinghai Bureau of Geology and Mineral Resources* (*QBGMR*) [1989a, 1989b]), showing sample locations and published magnetostratigraphic section [*Liu et al.*, 2001, 2003]. Inset map of the Tibetan orogen shows location of geologic map. Chronostratigraphic divisions indicated on geologic units are N_2: Pliocene, N_1: Miocene, E_3: Oligocene, E_{1-2}: Paleocene-Eocene, K_2: Upper Cretaceous, T_3: Late Triassic, T_2: Middle Triassic, and P_2: Guadalupian. Lettered locations in purple boxes correspond to photographs in Figure 4, except for location F which has no corresponding photo.

et al., 2012]. The stratigraphic relationships between the Fenghuoshan, Tuotuohe, and Yaxicuo Groups are a subject of debate, discussed more thoroughly below.

Subordinate volcanic deposits are preserved within, and depositionally on, the Fenghuoshan Group throughout the central Hoh Xil Basin. Within the Fenghuoshan Range, volcanic tuff layers interbedded within the Fenghuoshan Group are rare but present. Tuff and rhyodacitic (?) lava flows, which are interbedded within deformed fluvial red beds mapped as the lower Fenghuoshan Group, are exposed in an ~15 km wide syncline to the southwest of the Fenghuoshan Range (Figure 1) [*QBGMR*, 1989b]. Near the southern margin of the Fenghuoshan Range, subhorizontal basalt flows and associated ash layers are locally exposed and unconformably overlie steeply dipping beds of the Fenghuoshan Group (Figure 1).

In addition to volcanic deposits, syenitic and granitic plutonic bodies are interpreted to have intruded into previously deformed Fenghuoshan and Yaxicuo Group strata [*Wu et al.*, 2007; unpublished data cited in *Cyr et al.*, 2005]. The age constraints provided by these intrusive bodies are discussed below.

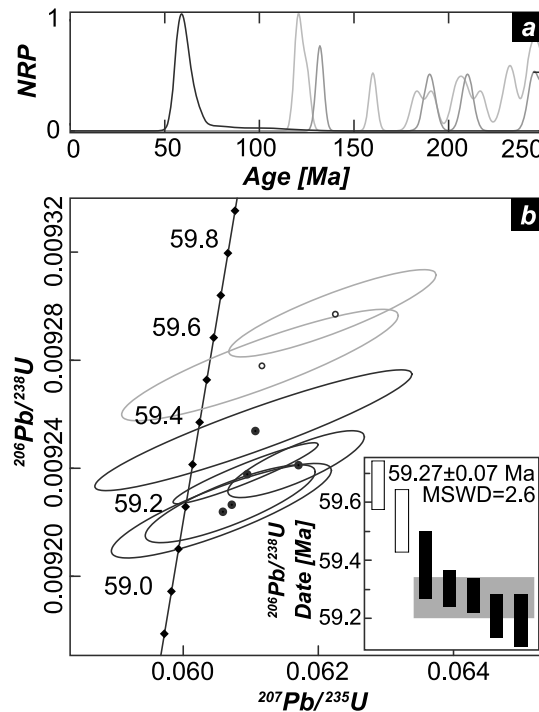## 3. New Age Constraints

3.1. Biostratigraphy

Biostratigraphic data can provide useful constraints on the depositional age of sedimentary strata; however, the robustness of age constraints is dependent on the level of detail and completeness of the data collected. Within the Hoh Xil Basin, detailed biostratigraphic studies of the Tuotuohe, Yaxicuo, and Wudaoliang Groups provide fossil identification, stratigraphic position, and relative abundance of 252 unique taxa, yielding reliable age control. These studies suggest depositional ages for the Tuotuohe, Yaxicuo, and Wudaoliang Groups of Paleocene to early Oligocene, Oligocene, and early Miocene, respectively [*Liu and Wang*, 2001a; *Liu et al.*, 2001, 2003; *Z. Duan et al.*, 2007; *Q. Duan et al.*, 2007; *Q. Duan et al.*, 2008; *Li et al.*, 2012]. Biostratigraphic data available for the Fenghuoshan Group, however, are less complete, and derived interpretations of its depositional age are subject to debate. Several studies interpret the flora and fauna as suggesting a Late Cretaceous depositional age [*Zhong*, 1989; *Li and Yuan*, 1990; *Ji*; 1994; *An*, 2004], while others infer a Paleocene-Oligocene depositional age [*Smith and Xu*, 1988]. Here we compile published biostratigraphic data collected from the Fenghuoshan Group to reevaluate its potential for providing robust age control [*Zhong*, 1989; *QBGMR*, 1989a, 1989b; *Li and Yuan*, 1990; *Ji*, 1994; *Liu et al.*, 2003; *An*, 2004].

Compiled biostratigraphic data from the Fenghuoshan Group include 68 taxa identified throughout the unit. Stratigraphic information of fossil occurrences throughout the section is reported and plotted in Figure 2a. The detail of stratigraphic localities reported for each identified fossil varies between studies, ranging from tens to thousands of meters, and relative abundances of individual taxa are not reported. Most studies from which we compile biostratigraphic data do not span the entire stratigraphic thickness of the Fenghuoshan Group but rather focus on the lower ~1700 m of the unit. Therefore, the stratigraphic range over which taxa exist may not be fully realized. Age ranges for each individual fossil lineage identified in Fenghuoshan Group strata, as well as fossils identified in overlying Tuotuohe, Yaxicuo, and Wudaoliang Group strata, were determined from published global accounts of fossil occurrences (Figure 2b; Tables S1–S5 in the supporting information). For any individual fossil that was ascribed two or more noncontiguous age ranges, the range used in this study is the inclusive span of all of the age ranges.

The lack of published fossil abundances and the coarse stratigraphic information available for many of the fossils identified within the Fenghuoshan Group limits our ability to construct detailed biozones throughout the stratigraphic unit to assess the depositional age and would potentially result in misconstrued fossil assemblages that either omit important taxa for which there is limited stratigraphic information or place emphasis on taxa that are relatively scarce. Instead, we consider the depositional age range of the Fenghuoshan Group to span from the youngest first occurrence to the oldest last occurrence of all fossils identified. Using this approach, the depositional age range for the Fenghuoshan Group lies between 100 and 56 Ma (Cenomanian-Ypresian; Figure 2b). All fossils are equally weighted, which potentially broadens our assessment of the depositional age range of the Fenghuoshan Group. One fossil, *Hornichara maslovi*, does not lie within this age range and is identified as Pliocene in age. Possible explanations for this misfit include fossil misidentification or that *Hornichara maslovi* has a broader age range than previously recognized.

We attempt to further refine the depositional age of the Fenghuoshan Group by identifying index fossils that are known regionally and globally to be age restrictive and by comparing fossil taxa of the Fenghuoshan Group with the overlying Tuotuohe, Yaxicuo, and Wudaoliang Groups (Figure S1). Ostracods *Eucypris* and *Quadracypris* were identified in the lower Fenghuoshan Group (Figure 2a) and are also found together in Cenomanian-Santonian (99.6–83.6 Ma) fossil assemblages from southern China [*Ye*, 1994]. Similarly, ostracod *Kaitunia* and pollen fossil *Schizaeoisporities* were both identified in lower the Fenghuoshan Group (Figure 2a) and are known to occur coevally in Upper Cretaceous strata from the Hengyang and Songliao basins [*Mateer and Chen*, 1992; *Zhang et al.*, 2007]. Sporopollen fossils *Jiaohepollis*, *Pristinuspollenites*, *Pseudopicea*, *Biretisporites*, *Concavisporites*, and *Converrucosisporites* were identified within the Fenghuoshan Group and are reportedly Cretaceous taxa that disappear after the Maastrichtian (< 65 Ma) [*Chen*, 1988; *Li and Liu*, 1994; *Li et al.*, 2011]. In the Jiansu Basin, *Schizaeoisporites* is identified as an index fossil for the Upper Cretaceous

Figure 2. Biostratigraphic data ranked by earliest occurrence in the Fenghuoshan Group [*QBGMR*, 1989a, 1989b; *Zhong*, 1989; *Li and Yuan*, 1990; *Ji*, 1994; *Liu et al.*, 2003; *An*, 2004]. (a) Stratigraphic column on the left [*Zhong*, 1989], along with individual taxa and their reported stratigraphic occurrences. Thick lines indicate stratigraphic ranges over which the fossils have been identified. Thin lines indicate the intervening statigraphic range between reported fossil occurrences. (b) Global age ranges for individual fossil lineages are shown as vertical black lines. Lineage age ranges are from published accounts of fossil occurrences (citations and lineage age ranges provided in the supporting information, Tables S1–S5). Horizontal grey bar indicates the biostratigraphically constrained age range of 56 to 100 Ma from these fossils by the overlap of the oldest last occurrence and the youngest first occurrence.

Tiazhou Formation and occurs along with sporopollen taxa *Gabonisporis*, *Pterisisporites*, *Deltoidospora*, *Classopollis*, *Exesispollenites*, *Ephedripites*, *Podocarpidites*, *Cedripides*, *Pinuspollenites*, and *Inaperturopollenites* [*Mateer and Chen*, 1992; *Song et al.*, 1995] all of which have been identified within the Fenghuoshan Group. Furthermore, *Densoisporities*, *Gabonisporites*, and *Exesipollenites*, which are present in the Fenghuoshan Group but absent from Tuotuohe and Yaxicuo Groups [*Q. Duan et al.*, 2007; *Z. Duan et al.*, 2007; *Duan et al.*, 2008], are common in Upper Cretaceous strata but absent from Tertiary strata from southeast China [*Song and Huang*, 1997]. Charophyte taxa *Peckichara* is found in Upper Cretaceous to Eocene strata [*Van Itterbeeck et al.*, 2007], and fossils *Peckichara subsphaerica*, *Rhabdochara*, *Gyrongona*, and *Obtusochara* found in the Fenghuoshan Group are similar to assemblages of Paleocene and early Eocene strata in the Sanshui Basin [*Chen and Xie*, 2011]. *Juglans*, *Betula*, *Ostrya*, and *Alnus* pollen, which evolved in middle Eocene time [*Crane and Stockey*, 1987; *Manchester*, 1987], are absent in the Fenghuoshan Group but are present in the overlying Tuotuohe, Yaxicuo, and Wudaoliang Groups. This may suggest that deposition of the Fenghuoshan Group ceased before the middle Eocene. Overall, biostratigraphic data from the Fenghuoshan Group share many taxa with Upper Cretaceous nonmarine strata in

Figure 3. U-Pb zircon geochronologic constraints on the depositional age of the Fenghuoshan Group. (a) Normalized relative probability (NRP) plot of Fenghuoshan Group detrital zircon dates (grey; $n = 78$) [*Dai et al.*, 2012] and LA-ICPMS U-Pb zircon dates (black; $n = 56$; this study) from a tuff interbedded within the Fenghuoshan Group. (b) Concordia diagram of zircons from the same tuff. Inset is a ranked age plot showing agreement between five youngest dates with a mean CA-TIMS zircon date of 59.27 Ma. Grey bar indicates overlap of five youngest zircon dates.

China, as well as some similarities with nonmarine Paleocene and early Eocene strata. We suggest that our biostratigraphically constrained Cenomanian-Ypresian depositional age for the Fenghuoshan Group is relatively accurate and at the very least provides a rough depositional age constraint for more precise age dating, discussed below.

3.2. Uranium-Lead Methods

High-precision U-Pb dates were acquired from a volcanic tuff interbedded in the Fenghuoshan Group (Figure 1) using chemically abraded thermal ionization mass spectrometry (CA-TIMS) at the Boise State University Isotope Geology Laboratory. Zircon separates were obtained using standard magnetic and density techniques, mounted in epoxy, and polished to expose crystal cores. Because cathodoluminescence (CL) images of the zircon crystals suggested the possibility of crystal zonation and inherited cores (Figure S2), 56 zircon grains were dated using laser ablation inductively coupled plasma mass spectrometry (LA-ICPMS) prior to high-precision CA-TIMS analysis.

U-Pb spot analyses were completed using a ThermoElectron X-Series II quadrupole ICPMS and New Wave Research UP-213 Nd: YAG UV LA system with a spot diameter of 25 μm. Background count rates, which were measured before individual spot analyses, were subtracted from raw count rates. U-Pb dates were corrected for instrumental $^{206}Pb/^{238}U$ and $^{207}Pb/^{206}Pb$ ratio fractionation and calibrated using isotopic ratio measurements of a Plešovice zircon standard [*Sláma et al.*, 2008]. U-Pb age error includes counting statistic and background subtraction uncertainty. U-Pb dates and associated errors (2σ) are reported in Table S6 and compared to detrital U-Pb zircon ages from the Fenghuoshan Group (Figure 3a) [*Dai et al.*, 2012]. LA-ICPMS $^{206}Pb/^{238}U$ zircon dates are taken to give the best estimate of crystallization age for these relatively young zircons and range between 107 ± 7 and 56 ± 3 Ma. The faceted appearance of zircon crystals (Figure S2), similarity in zircon chemistry, exhibited by low Th/Y ratios and uniform steepness of middle to heavy rare earth element slopes (Figure S4 and Table S6) [e.g., *Rivera et al.*, 2013], and lack of overlap with detrital U-Pb zircon ages from the Fenghuoshan Group (Figure 3a) [*Dai et al.*, 2012] indicate that the U-Pb zircon ages from the tuff are from a single eruptive event and are unlikely to have experienced reworking postdeposition. The distribution in ages observed in LA-ICPMS analysis may be explained by xenocrystic contamination during eruption or loss of radiogenic Pb after zircon crystallization [*Schoene et al.*, 2010], and we note that the range in zircon U-Pb ages present in the tuff is consistent with the duration of magmatism in the Gangdese arc (Figure S5) [*Wen et al.*, 2008], suggesting a possible eruptive source. On the basis of zircon morphology and zonation based on CL images (Figure S2), 38 grains were determined to be autocrystic, while the remaining 18 were assumed to be xenocrystic. The weighted mean LA-ICPMS U-Pb age of the 38 autocrystic zircon grains is 58.8 ± 0.6 Ma (mean square weighted deviation (MSWD) = 2.4; Figure S3 and Table S6).

CA-TIMS U-Pb analyses were performed on the seven youngest zircon grains determined by LA-ICPMS analysis because the younger zircons are most likely to record the age of eruption [*Schoene et al.*, 2010]. The analyses were obtained using a methodology modified from *Mattinson* [2005] on a GV Isoprobe-T multicollector TIMS equipped with an ion-counting Daly detector. The zircon grains analyzed were removed from the epoxy mount for analysis and were heated to 900°C for 60 h and partially dissolved in 29 M HF at 180°C for 12 h. Grains were then placed in 3.5 M HNO$_3$ and ultrasonically cleaned. Each crystal grain was spiked with

EARTHTIME mixed ^{233}U-^{235}U-^{205}Pb tracer solution (ET535) and dissolved. U and Pb isotopes were separated from the zircon matrix [*Krogh*, 1973] and loaded onto single outgassed Re filaments and loaded for TIMS measurement [*Gerstenberger and Haase*, 1997]. U and Pb mass fractions were corrected using ^{233}U-^{235}U and ^{202}Pb-^{205}Pb isotopic ratios of the ET535 tracer solution, respectively. U-Pb dates and associated errors were calculated using procedures of *Schmitz and Schoene* [2007], ET535 tracer solution [*Condon et al.*, 2007], and U decay constants [*Jaffey et al.*, 1971] and corrected for initial ^{230}Th disequilibrium [*Crowley et al.*, 2007]. Ages with 2σ uncertainties are reported in Table S7 and illustrated in Figure 3b. ^{206}Pb/^{238}U zircon dates range between 59.66 ± 0.08 and 59.19 ± 0.09 Ma, with the five youngest dates obtained using CA-TIMS methodology yield a weighted mean date of 59.27 ± 0.07 Ma (MSWD = 2.4; Figure 3b and Table S7). We interpret this date to reflect the timing of volcanic tuff deposition.

3.3. Argon-Argon Methods

Existing constraints for the depositional age of the Fenghuoshan Group include syenite stocks and a granite porphyry that are interpreted to have intruded the previously deformed Fenghuoshan Group and Yaxicuo Group strata and are dated using ^{40}Ar/^{39}Ar methods at 28.6 ± 0.3 and U-Pb zircon methods at 27.6 ± 0.5 Ma, respectively [*Wu et al.*, 2007; D. B. Rowley, unpublished data]. We sampled a rhyodacite, which we interpret as a lava flow, interbedded with fluvial red beds that are mapped as the lower Fenghuoshan Group (unit K_{2fn}^a) [*QBGMR*, 1989b], for syndepositional age control (Figures 1 and 4a). Additionally, two undeformed basalt flows that overlie steeply dipping Fenghuoshan Group beds were collected near the southern margin of the Fenghuoshan Range for postdepositional age control (Figures 1 and 4e). Ages were measured using biotite ^{40}Ar/^{39}Ar dating techniques at the University of Michigan Argon Geochronology Laboratory. Bedrock samples were crushed and sieved to a particle size range of 250–1000 μm. The magnetic mineral fraction of the crushed sample was obtained using a Frantz magnetic separator and then shaken manually over a Mylar plastic sheet to concentrate biotite by static force. Biotite crystals for each sample were handpicked under a microscope from the concentrate to ensure purity. The biotite was then packed into pure Al foil and subjected to irradiation for 30 h at the McMaster Nuclear Reactor at McMaster University in packages mc35 and mc40. MMHb-1 was used as a standard with an assumed age of 520.4 Ma [*Samson and Alexander*, 1987]. Biotite was extracted from packets after irradiation and step heated with a Coherent Innova 5 W continuous argon ion laser. A VG1200S mass spectrometer with a Daly detector was used for Ar isotope measurement. Fusion system blanks were run every five fusion steps, and blank levels from ^{36}Ar through ^{40}Ar were subtracted from gas fractions. Corrections were made for the decay of ^{37}Ar and ^{39}Ar, K, Ca, and Cl interfering nucleogenic reactions and the production of ^{36}Ar from ^{36}Cl decay. A zero-aged artificial glass sample was used to correct for interfering reactions producing ^{40}Ar. We use the error-weighted average of the plateau age, which corresponds to the flattest portion of the apparent age spectrum, as the best estimate for timing of emplacement. ^{40}Ar/^{39}Ar analysis of the rhyodacitic lava yielded a date of 33.46 ± 0.24 Ma (Figure 5a; MSWD = 0.39). The upper and lower basalt flows are dated at 26.46 ± 0.23 Ma (MSWD = 0.63) and 27.33 ± 0.1 (MSWD = 0.76), respectively (Figures 5b and 5c).

4. Chronological Interpretations

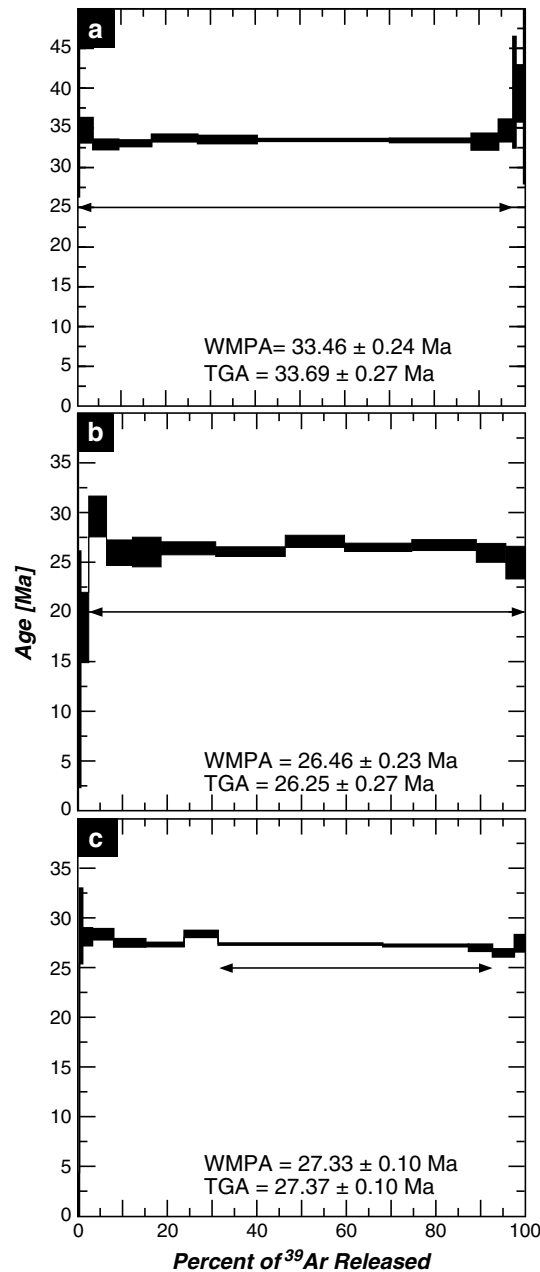### 4.1. Revised Age of the Fenghuoshan Group

As previously discussed, the depositional age of the Fenghuoshan Group is debated. Biostratigraphic studies have led to the interpretation that the Fenghuoshan Group is Late Cretaceous [*Zhong*, 1989; *Li and Yuan*, 1990; *Ji*; 1994; *An*, 2004] or Paleocene to early Eocene in age [*Smith and Xu*, 1988], based largely on pollen, ostracod, gastropod, and charophyte fossils. Conversely, magnetostratigraphic studies suggest an Eocene to Oligocene (51–31 Ma) age for the Fenghuoshan Group [*Liu et al.*, 2001, 2003]. This latter interpretation has been principally adopted by studies over the last decade as the depositional age of the Fenghuoshan Group [*Harrison et al.*, 1992; *Cyr et al.*, 2005; *C. Wang et al.*, 2008; *Quade et al.*, 2011; *Dai et al.*, 2012].

Interpreting the age of the Fenghuoshan Group is also complicated by a lack of consensus on the lateral distribution of the Fenghuoshan Group, and its stratigraphic relationship with the lithologically similar Tuotuohe Group. One interpretation of these two units is that they were deposited synchronously in two adjacent depositional basins (the Fenghuoshan subbasin and Tuotuohe subbasin of the Hoh Xil Basin) and thus are age equivalent [*Liu et al.*, 2005; *Li et al.*, 2012]. An alternate interpretation is that the Tuotuohe Group is younger than, and unconformably overlies, the Fenghuoshan Group [*Zhong*, 1989; *QBGMR*, 1989a, 1989b;
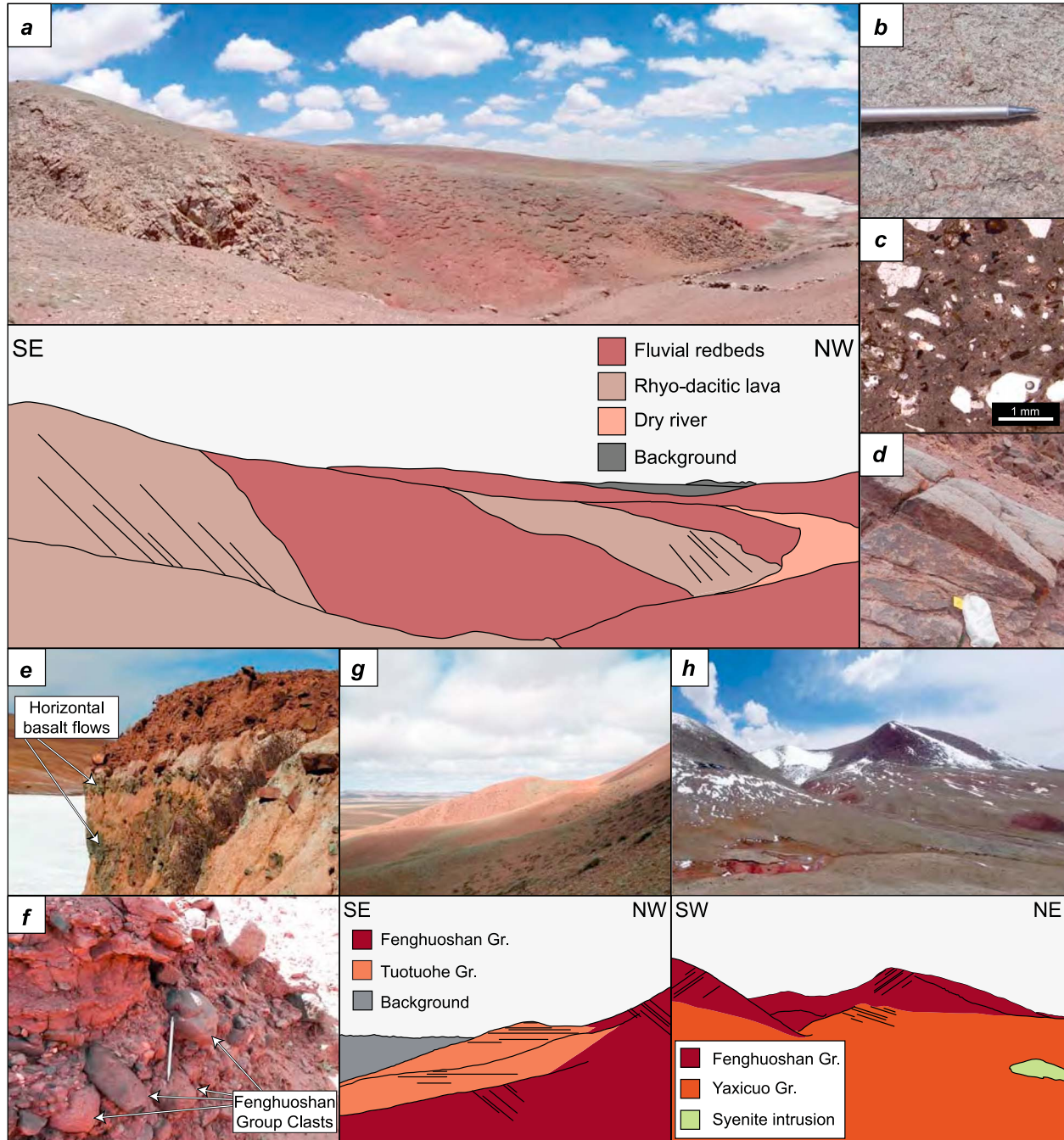
Figure 4. Field photographs, thin section photographs, and interpretive sketches of key geologic relationships of both extrusive volcanic rocks and between the Fenghuoshan Group and other Cenozoic sedimentary units. (a) Rhyodacitic lava flow interbedded with fluvial red beds, which have been mapped as the lower Fenghuoshan Group (Figure 1, location A) [*QBGMR*, 1989b]. Approximate bedding orientation is shown by horizontal lines. (b) Field photo of rheomorphic banding observed in rhyodacitic lava flow. (c) Thin section photograph of rhyodacite showing a large percentage of finely crystalline groundmass. (d) Field photo of eutaxitic foliation observed in rhyodacite that is subparallel to surrounding sedimentary bedding orientation. (e) Horizontal basalt flows that overlie deformed Fenghuoshan Group strata near Erdagou (Figure 1, location B). (f) Tuotuohe Group conglomerate containing a large proportion of rounded cobbles of the Fenghuoshan Group (Figure 1, location C). (g) Angular unconformity between the Fenghuoshan and Tuotuohe Groups along the southern margin of the Fenghuoshan Range with bedding orientations indicated by straight lines (Figure 1, location D). (h) Angular unconformity between the Fenghuoshan and Yaxicuo Groups along the northern margin of the Fenghuoshan Range (bedding orientations indicated by straight lines; Figure 1, location E).

Figure 5. ^{40}Ar/^{39}Ar geochronologic constraints on the depositional age of the Fenghuoshan Group. (a) ^{40}Ar/^{39}Ar spectra for biotites separated from a rhyodacite lava flow interbedded within red beds that are mapped as the lower Fenghuoshan Group (Figure 1). (b and c) ^{40}Ar/^{39}Ar release spectra from biotite separated from horizontal basalt lava flows that unconformably overlie the Fenghuoshan Group near Erdaguo. Sample 11UMT17-A (Figure 5b) and sample 11UMT17-B (Figure 5c). TGA: total gas age. WMPA: weighted mean plateau age.

Ji, 1994; *An et al.*, 2004]. We will address the stratigraphic relationship between these two units below but focus here on the age of the Fenghuoshan Group from observations that are solely derived from exposures in the Fenghuoshan Range, with the exception of one set of biostratigraphic constraints that were taken from exposures both in and to the south of the Fenghuoshan Range [*Ji*, 1994].

4.1.1. Age of the Fenghuoshan Group in the Fenghuoshan Range

Our new 59.27 Ma U-Pb zircon age from a tuff interbedded with the Fenghuoshan Group strata require that the deposition of these strata is, at least in part, Paleocene in age. The Oligocene ages we have determined of basalt flows overlying the Fenghuoshan Group, combined with existing detrital zircon age spectra [*Dai et al.*, 2012], are used as absolute upper and lower constraints on the depositional age of the Fenghuoshan Group. These constraints place deposition of the Fenghuoshan Group at 121–27 Ma. The compiled biostratigraphic data set suggests a more narrow depositional age range of 100–56 Ma (Figure 2).

Based on these depositional age constraints, we provide a revised correlation of the published magnetostratigraphic record to the geomagnetic polarity timescale (Figure 6) [*Zhong*, 1989; *QBGMR*, 1989a, 1989b; *Li and Yuan*, 1990; *Ji*, 1994; *Liu et al.*, 2001; *An*, 2004; *Dai et al.*, 2012]. The magnetostratigraphic polarity pattern published by *Liu et al.* [2003] combined sedimentary sections of the Fenghuoshan and Yaxicuo Groups. In our revision, we chose not to include magnetostratigraphic data from the Yaxicuo Group in our reinterpretation. Field evidence from the Fenghuoshan Range indicates an unconformable contact between the Fenghuoshan Group and the overlying Yaxicuo Group. Additionally, magnetostratigraphic samples for the Fenghuoshan and Yaxicuo Groups were collected from different locations within the Hoh Xil Basin [*Liu et al.* 2003]. Since conformable deposition between these two magnetostratigraphic sections cannot be verified, we argue that the Yaxicuo Group magnetostratigraphy must be correlated to the geomagnetic polarity timescale independent of any correlations made for the Fenghuoshan Group. Because the Yaxicuo Group magnetostratigraphic data contain few magnetic reversals and no precise

independent age constraints [*Liu et al.* 2003], unique correlation with the geomagnetic polarity timescale (GPTS) is not possible at this time.

A revised polarity zonation for the Fenghuoshan Group magnetostratigraphic polarity pattern was devised from paleomagnetic data published by *Liu et al.* [2003] (Figures 6 and S6). Polarity zones were defined by two
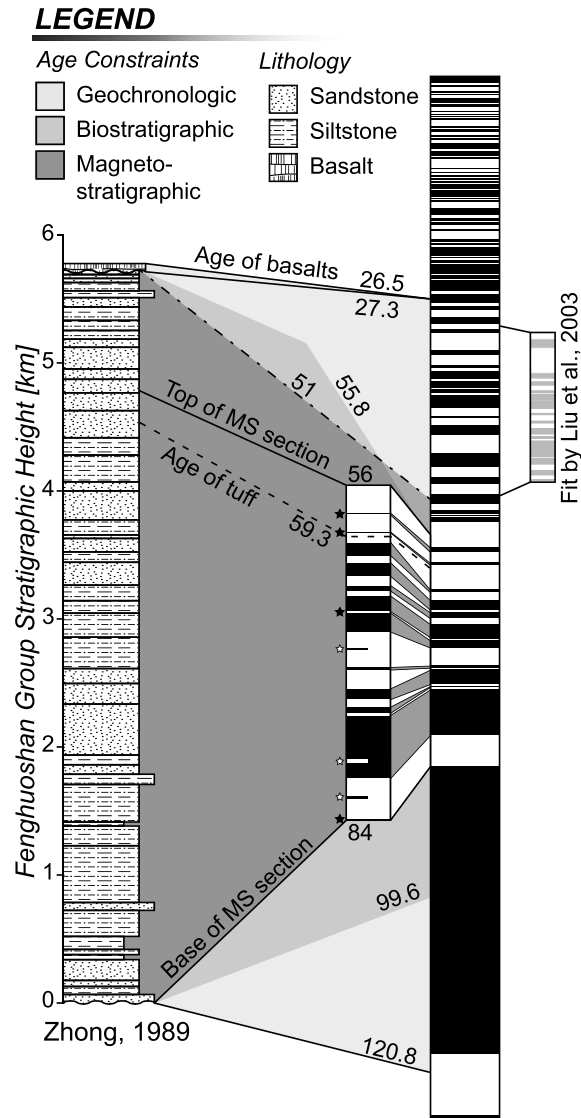
Figure 6. Compiled biostratigraphic and radiometric age constraints for the Fenghoshan Group, along with a revised magnetostratigraphic fit and stratigraphic column (as measured by *Zhong* [1989]). The possible depositional age range for Fenghuoshan Group strata, constrained by detrital zircon U-Pb age spectra [*Dai et al.*, 2012] and unconformably overlying basaltic lava flows (this study) is shown in light grey. The depositional age constraints inferred from the biostratigraphic compilation (Figure 2) is shown in medium grey. The depositional age as constrained from magnetostratigraphy is shown by solid lines. The inferred complete depositional age range of the Fenghuoshan Group, as extended by sediment accumulation rate (Figure 7), is shown in dark grey. The radiometrically dated interbedded volcanic tuff is shown as a dashed line. A previous magnetostratigraphic fit, as published by *Liu et al.* [2003], is shown to the right of the geomagnetic timescale [*Gradstein et al.*, 2012].

or more samples with sequential characteristic remnant magnetization (ChRM) directions that are clearly normal or reverse in polarity. Published magnetostratigraphic data from the Fenghuoshan Group are correlated to the *Gradstein et al.* [2012] GPTS using our new age constraints as depositional bounds. We find that the Fenghuoshan Group magnetostratigraphic polarity pattern is best correlated to the GPTS pattern between magnetozones C34n and C24r (Figures 6 and S6). Four individual magnetozones in the GPTS pattern are not resolved in our revised polarity zonation for the Fenghuoshan Group. By revisiting the Fenghuoshan Group paleomagnetic data, we find that the unresolved GPTS magnetozones are, in fact, recorded, but only with one datum. We include these four magnetozones in the analysis of the Fenghuoshan polarity pattern on the basis that paleomagnetic sampling was conducted at 10–12 meter intervals, depending on lithology [*Liu et al.*, 2003], and may have been coarse enough to capture short polarity intervals with only a single sample. Single-datum magnetozones included in the Fenghuoshan Group polarity pattern are denoted in Figures 6 and S6 with black stars. In addition to magnetozones that may be represented by single ChRM measurements, we find that three magnetozones in our reinterpreted polarity pattern are not present in the GPTS. All three uncorrelated magnetozones are defined by two data points that may constrain short intervals and are denoted with white-filled stars in Figures 6 and S6. Several explanations for minor polarity pattern mismatch are that thin magnetozones observed in the Fenghuoshan Group paleomagnetic data represent short-interval subchrons that are not published in the *Gradstein et al.* [2012] GPTS, that the primary ChRM directions are fully overprinted such that the recorded paleomagnetic signal does not reflect the true geomagnetic field direction at the time of deposition, or that these specific samples and results are of lesser quality. Without first-hand knowledge of sample quality, resolution, and rock magnetic properties, it is difficult to determine which explanation is likely for mismatched polarity zones; however, we note that these mismatches are relatively minor compared to the overall magnetic polarity stratigraphy correlation and that the revised correlation satisfies the new age constraints required for correlation and age interpretation. We exclude the three unmatched magnetozones from further analysis.
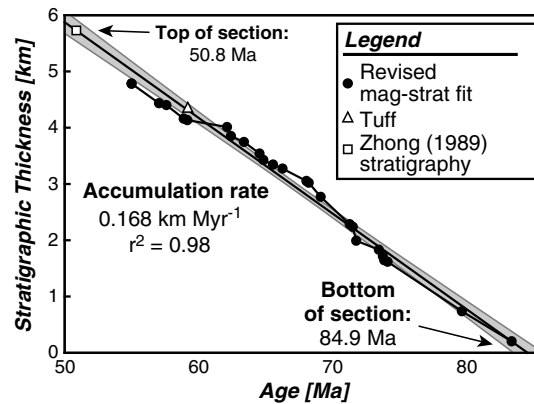
Figure 7. Sediment accumulation rate of the Fenghuoshan Group, based on stratigraphic thickness and revised magnetos-tratigraphic age (black dots; Figure 6). The sediment accumulation rate is calculated using linear least squares regression, with 95% confidence interval shaded in grey. White squares are the top and bottom of the Fenghuoshan Group stratigraphic section measured by *Zhong* [1989], which documents over 5.7 km of continuously deposited Fenghuoshan Group strata. The grey triangle shows the age and assumed stratigraphic thickness of the radiometrically dated volcanic tuff (Figures 3 and 6).

The base of *Liu et al.*'s [2003] magnetostratigraphic section was measured ~184 m below the oldest reversal (C34n to C33r), and the top of the section was measured ~380 m above the youngest reversal (C25n to C24r); thus, the depositional age range of the Fenghuoshan Group extends above and below chrons C25n and C33n, respectively. Furthermore, while the base of the Fenghuoshan Group corresponds to the lowest sample collected for magnetostratigraphic analysis, the full stratigraphic extent of the Fenghuoshan Group extends over 900 m beyond the highest magnetostratigraphic sample collected [*Zhong*, 1989]. Therefore, the upper bound of the Fenghuoshan Group depositional age range lies ~1291 m above the youngest polarity reversal recorded by paleomagnetic data [*Liu et al.*, 2003]. Using a sediment accumulation rate derived from linear regression through our reinterpretation of the magnetostratigraphic data (Figure 7), we extrapolate the depositional age of the base (~184 m below the oldest recorded reversal) and of the top (~1291 m above the youngest recorded reversal) of the Fenghuoshan Group strata. This extrapolation provides a depositional age range for the Fenghuoshan Group of 85 to 51 Ma (Figures 6 and 7). We therefore propose that the Fenghuoshan Group was deposited from Late Cretaceous (~Santonian/Campanian boundary) to early Eocene (late Ypresian) time.

4.1.2. Age of the Fenghuoshan Group (?) in the Tuotuohe Region

In the Tuotuohe region, we collected a rhyodacite lava flow interbedded within deformed red beds in order to constrain the depositional age of those units. Regional geologic maps [*QBGMR*, 1989a] indicate that the rhyodacite lava is interbedded within the lower Fenghuoshan Group (unit K_{2fn}^{a}; Figures 1 and 4a). The $^{40}Ar/^{39}Ar$ age determined for the rhyodacite is 33.47 Ma, thus implying that map unit K_{2fn}^{a} is not the same age in the Tuotuohe Basin as in the Fenghuoshan Range. The radiometric age from the rhyodacite lava more closely reflects the biostratigraphic age constraints from strata identified as the Tuotuohe and Yaxicuo Groups. Three possibilities arise from this age: (1) the depositional age range of the Fenghuoshan Group extends from the Late Cretaceous into at least the earliest Oligocene and that the stratigraphy of the Hoh Xil Basin exhibits considerable lateral variation; (2) Fenghuoshan Group strata (as defined from localities in the Fenghuoshan Range) are not exposed in the Tuotuohe subbasin and that the rhyodacitic flow was collected from lithologically similar Tuotuohe Group strata; or (3) we have misinterpreted the rhyodacite as an extrusive lava flow, when it is instead intruded into Fenghuoshan Group strata.

In the third possibility, the rhyodacite may be a sill that has intruded the Fenghuoshan Group, an interpretation that would be in agreement with regional geologic mapping [*QBGMR*, 1989a]. However, the rhyodacite displays a number of characteristics that are indicative of a lava flow, including rheomorphic banding (Figure 4b), autobrecciation at the flow margins, and a large percentage (71.2%) of groundmass (Figure 4c), which is based on a point count of 1000 points. Although such features are not unique to extrusive flows, they are rarely reported in igneous intrusions, even those known to be hypabyssal [e.g., *Orth and McPhie*, 2003]. The agreement between the orientation of eutaxitic foliation in the rhyodacite (Figure 4d) and the orientation of local bedding is also suggestive of an extrusive origin. Nonetheless, if this igneous body is, in fact, intrusive, then the $^{40}Ar/^{39}Ar$ age provides only a minimum depositional age for these red bed strata and does not constrain the timing of deformation in this region. Regardless, the biostratigraphic, geochronologic, and reinterpreted magnetostratigraphic data, described above, imply that the Fenghuoshan Group in the Fenghuoshan Range was deposited in Late Cretaceous to early Eocene time, and the stratigraphic relationships between the Tuotuohe and Fenghuoshan Groups, described below, imply that they are separate geologic units. All of these data underscore the difficulty in constraining absolute

Legend

Wudaoliang Group

Yaxicuo Group

Tuotuohe Group

Fenghuoshan Group

a

b

c

d
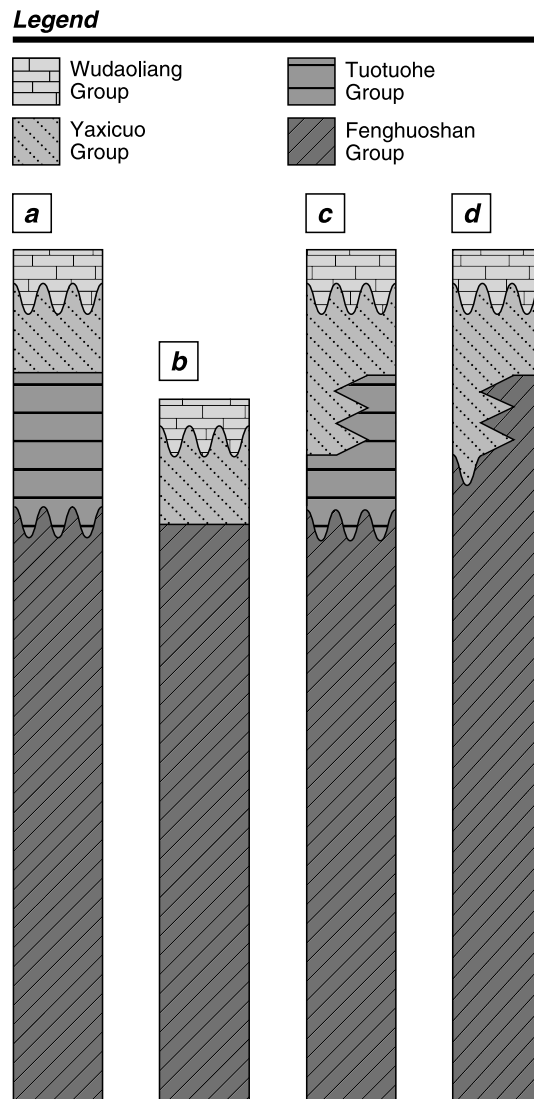
Figure 8. Stratigraphic relationships of the Fenghuoshan, Tuotuohe, Yaxicuo, and Wudaoliang Groups proposed by (a) *Zhong* [1989], *Li and Yuan* [1990], *Ji* [1994], *An* [2004], (b) *Liu et al.* [2001], 2003, 2005, and *Li et al.* [2011], and (c and d) this study.

depositional age of continental strata on the Tibetan Plateau and the need for additional work to better define the relationships between Cenozoic units in the Hoh Xil region.

5. Stratigraphy of the Hoh Xil Basin

Previous studies conducted in the Hoh Xil Basin have inferred several contradictory possibilities for the stratigraphic relationships of the nonmarine sedimentary units. One argument, briefly mentioned above, revolves around whether the Fenghuoshan Group and Tuotuohe Group are lithostratigraphically and chronostratigraphically equivalent. Geologic maps at a scale of 1:200,000 in the Fenghuoshan Range and Tuotuohe region divide Late Cretaceous to Miocene nonmarine sedimentary rocks into four distinct lithologic units: the Fenghuoshan, Tuotuohe, Yaxicuo, and Wudaoliang Groups [*QBGMR*, 1989a, 1989b]. This interpretation of the regional geology of the Hoh Xil Basin contrasts with several local lithostratigraphic and magnetostratigraphic studies of these rocks that consider the Fenghuoshan Group and Tuotuohe Group to be the same stratigraphic unit [*Liu et al.*, 2005; *C. Wang et al.*, 2008; *Li et al.*, 2012]. Furthermore, there is disagreement on the depositional boundaries between lithostratigraphic units. The regional geologic maps and stratigraphic studies that consider the Fenghuoshan and Tuotuohe Groups to be distinct units also consider the Tuotuohe and Yaxicuo Groups to be unconformably deposited on Fenghuoshan Group strata (Figure 8a) [*Zhong*, 1989; *Li and Yuan*, 1990; *Ji*, 1994; *An*, 2004]. Conversely, magnetostratigraphic and lithostratigraphic studies from both the Fenghuoshan Range and Tuotuohe Basin report that Yaxicuo strata

conformably overlie the Fenghuoshan Group (Figure 8b) [*Liu et al.*, 2001, 2003, 2005; *Li et al.*, 2012]. Resolving these contradictions in stratigraphic relationships is crucial, as the magnetostratigraphic age interpretations of the Tuotuohe and Yaxicuo Groups rely on stratigraphic correlation with magnetostratigraphic record from the Fenghuoshan Range and the interpretation of depositional contacts between stratigraphic units. Our observations, discussed below, support the interpretation that the Fenghuoshan, Tuotuohe, Yaxicuo, and Wudaoliang Groups are distinct stratigraphic units and that the Tuotuohe and Yaxicuo Groups are unconformably deposited on Fenghuoshan Group strata.

5.1.1. Tuotuohe Group

The Tuotuohe Group is composed of sandstone and conglomerate and shows evidence for moderate postdepositional deformation [*Li et al.*, 2012]. The Tuotuohe and Fenghuoshan Groups are lithostratigraphically similar in many locales. However, to the south of the Fenghuoshan Range, clasts of the Fenghuoshan Group are incorporated within gently tilted Tuotuohe Group conglomerate (Figure 1, location C; Figure 4f). Along the southern margin of the Fenghuoshan Range, the Tuotuohe Group is deposited in angular unconformity on the lower Fenghuoshan Group, which is dipping steeply relative to Tuotuohe Group strata (Figure 1, location

D; Figure 4g). Both units are uplifted along a north dipping thrust fault. These observations suggest that the Tuotuohe and Fenghuoshan Groups are distinct stratigraphic units and that the Tuotuohe Group was deposited after the Fenghuoshan Group was deformed, but before deformation within the Hoh Xil Basin ceased.
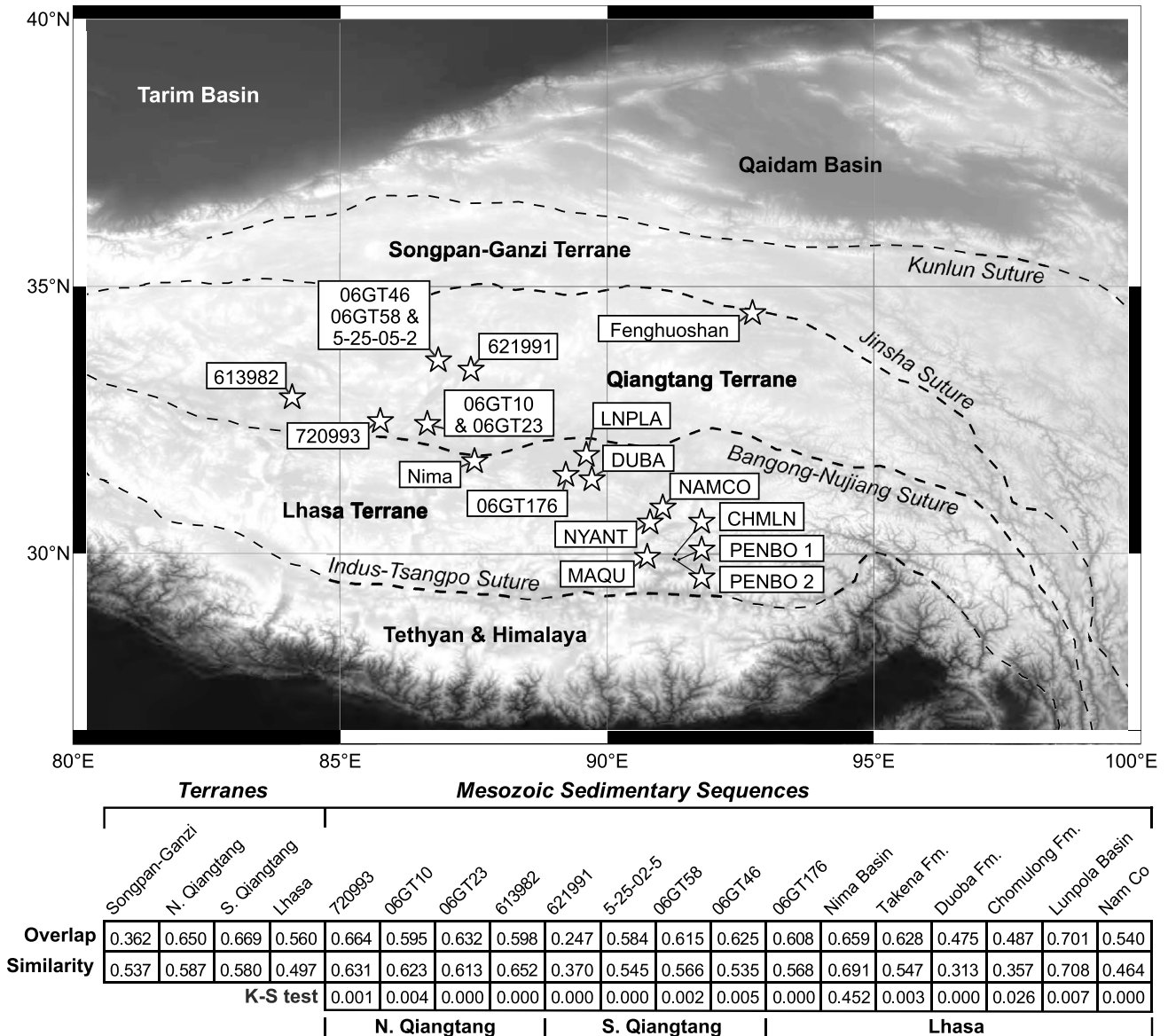
5.1.2. Yaxicuo Group

The Yaxicuo Group is exposed on either side of the Fenghuoshan Range as moderately deformed orange-buff-colored strata composed of fluvial-lacustrine mudstone, siltstone, and sandstone with interbedded gypsum and lacustrine carbonate (Figure 1) [*Liu and Wang*, 2001a; *Liu et al.*, 2005; *Li et al.*, 2012]. On either side of the Fenghuoshan Range, the Yaxicuo Group comes in contact with the lower unit of the Fenghuoshan Group (Figure 1). To the north of the Fenghuoshan Range, an angular unconformity between the Fenghuoshan and Yaxicuo Groups is evidenced by strikingly different bedding orientations between these units (Figure 1, location E; Figure 4h). The northern margin of the Fenghuoshan Range (Figure 1, location E) is marked by an abrupt geomorphic change from steep slopes, in which the lower Fenghuoshan Group strata are exposed, to low-angle slopes, in which the Yaxicuo Group is exposed. Bedding orientations in either unit do not support conformable deposition, but outcrop quality is poor, the contact is obscured, and it is possible that the northern margin of the Fenghuoshan Range is a thrust fault, in which lower Fenghuoshan Group strata is thrust northward over the Yaxicuo Group. A study in the Tuotuohe subbasin, to the south of the Fenghuoshan Range, describes Yaxicuo strata conformably overlying the Fenghuoshan Group [*Liu et al.*, 2005]. However, detailed regional geologic maps that differentiate between the Fenghuoshan and Tuotuohe Groups indicate that the Yaxicuo Group is deposited on Tuotuohe Group strata at the study locality. These observations suggest that at least locally, the Yaxicuo Group is conformable with the underlying Tuotuohe Group but is regionally deposited unconformably over the Fenghuoshan Group.

5.1.3. Stratigraphic Interpretation

As mentioned above, previous studies have suggested two stratigraphic interpretations for nonmarine units in the Hoh Xil Basin (Figures 8a and 8b) [*Zhong*, 1989; *Li and Yuan*, 1990; *Ji*, 1994; *Liu et al.*, 2001, 2003, 2005; *An*, 2004; *Li et al.*, 2012]. However, based on our observed stratigraphic relationships and the biostratigraphically constrained depositional ages of the Tuotuohe and Yaxicuo Groups [*Z. Duan et al.*, 2007; *Q. Duan et al.*, 2007; *Duan et al.*, 2008], which suggest that there may be some chronological overlap between these units in early Oligocene time, we suggest two additional interpretations of the stratigraphy of the Hoh Xil Basin (Figures 8c and 8d). The first possibility is that the Tuotuohe and Fenghuoshan Groups are distinct stratigraphic units, that the Fenghuoshan Group is unconformably overlain by the Yaxicuo and Tuotuohe Groups, and that the lower Yaxicuo and the upper Tuotuohe Groups were synchronously deposited and represent lateral variability in depositional facies (Figure 8c). Alternatively, the Tuotuohe Group may represent continued, syndeformational deposition of the Fenghuoshan Group, in which growth strata produced the angular unconformities we observe along the northern and southern margins of the Fenghuoshan Range, while the Yaxicuo Group was synchronously deposited with the upper member of the Fenghuoshan Group (Figure 8d).

Of the four stratigraphic possibilities proposed in Figure 8, we favor the interpretation in which the Fenghuoshan Group and Tuotuohe Group are distinct stratigraphic units (Figure 8c). While the Fenghuoshan and Tuotuohe Groups are generally lithostratigraphically similar, several observations have led us to distinguish these groups as separate units. To the south of the Fenghuoshan Range, we have observed Tuotuohe Group conglomerate clasts composed of Fenghuoshan Group sandstone (Figure 4f). Along the southern margin of the Fenghuoshan Range, the Tuotuohe Group is composed of beige coarse-grained sandstone and is angularly unconformable with deep red fine- to medium-grained sandstone of the Fenghuoshan Group (Figure 4g). These observations imply that the Tuotuohe Group is a syntectonic unit that was deposited after the Late Cretaceous to earliest Eocene Fenghuoshan Group, from Eocene to early Oligocene time. While the Yaxicuo Group is reportedly conformable with the Tuotuohe Group in the Tuotuohe subbasin [*Li et al.*, 2011], the overlap of the Yaxicuo Group and Tuotuohe Group biostratigraphically determined age ranges [*Z. Duan et al.*, 2007; *Q. Duan et al.*, 2007; *Duan et al.*, 2008] may suggest coeval deposition and laterally shifting depositional facies in the early Oligocene. Finally, the Miocene Wudaoliang Group is unconformable with underlying stratigraphic units within the Hoh Xil Basin, according to our field observations, as well as observations made by others [*Liu et al.*, 2001, 2003; *Wu et al.*, 2008; *Li et al.*, 2012].

	Terranes				Mesozoic Sedimentary Sequences														
	Songpan-Ganzi	N. Qiangtang	S. Qiangtang	Lhasa	720993	06GT10	06GT23	613982	621991	5-25-02-5	06GT58	06GT46	06GT176	Nima Basin	Takena Fm.	Duoba Fm.	Chomulong Fm.	Lunpola Basin	Nam Co
Overlap	0.362	0.650	0.669	0.560	0.664	0.595	0.632	0.598	0.247	0.584	0.615	0.625	0.608	0.659	0.628	0.475	0.487	0.701	0.540
Similarity	0.537	0.587	0.580	0.497	0.631	0.623	0.613	0.652	0.370	0.545	0.566	0.535	0.568	0.691	0.547	0.313	0.357	0.708	0.464
K-S test					0.001	0.004	0.000	0.000	0.000	0.000	0.002	0.005	0.000	0.452	0.003	0.000	0.026	0.007	0.000
					N. Qiangtang				**S. Qiangtang**				**Lhasa**						

Figure 9. Comparison between detrital U-Pb zircon age spectra for the Fenghuoshan Group [*Dai et al.*, 2012] with four possible source terranes on the Tibetan Plateau (Lhasa, northern and southern Qiangtang, and Songpan-Ganzi) and 10 Mesozoic sedimentary sequences deposited across the Tibetan Plateau [*Bruguier et al.*, 1997; *Weislogel et al.*, 2006, 2010; *Leier et al.*, 2007b; *Kapp et al.*, 2007a; *Gehrels et al.*, 2011]. The map shows locations and sample names of Mesozoic sedimentary units compared to the Fenghuoshan Group (white stars). The table below shows the overlap, similarity, and K-S test values derived from comparison of the Fenghuoshan Group with each Tibetan terrane and Mesozoic sedimentary unit. Sutures delineate the terrane boundaries and are marked as dashed black lines [*Styron et al.*, 2010].

6. Source of the Fenghuoshan Group

To constrain possible source terranes for the Fenghuoshan Group, published detrital zircon U-Pb age spectra from the Fenghuoshan Group [*Dai et al.*, 2012] were compared to spectra from 10 Mesozoic sedimentary units from across the Tibetan Plateau [*Leier et al.*, 2007b; *Kapp et al.*, 2007a; *Gehrels et al.*, 2011], as well as detrital zircon age compilations from the Lhasa, southern Qiangtang, northern Qiangtang, and Songpan-Ganzi terranes [*Bruguier et al.*, 1997; *Weislogel et al.*, 2006, 2010; *Gehrels et al.*, 2011]. We used three statistical methods in this analysis: (1) measurement of overlap, which considers the age range overlap between two samples; (2) measurement of similarity, in which the proportions of overlapping ages are compared; and (3) the Kolmogorov-Smirnov test (K-S test) to determine the probability that detrital zircon age distributions are derived from the same parent population. For the first two tests, a value of 1.0 suggests perfect overlap and

similarity, whereas a value of 0.0 suggests no overlap or similarity [*Gehrels*, 2000]. For the K-S test, a *p* value of <0.05 indicates, within 95% confidence, that the two age spectra are from different sources [*Press et al.*, 1986].

Of the compiled zircon age spectra from Tibetan terranes compared to the Fenghuoshan Group, the northern and southern regions of the Qiangtang Terrane have the highest values of similarity and overlap, respectively (Figure 9). This provenance analysis suggests that the Qiangtang Terrane is the source of Fenghuoshan Group sedimentary rocks. This is consistent with paleocurrent indicators from the Fenghuoshan Group, which suggest northward flow directions [*Leeder et al.*, 1988; *Liu and Wang*, 2001b; *Liu et al.*, 2001; *Yi et al.*, 2008; *Li et al.*, 2012]. While we cannot statistically distinguish between the northern and southern sections of the Qiangtang Terrane, we interpret the presence of conglomerates in the Fenghuoshan Group as indicative of a proximal sedimentary source and thus infer that the Qiangtang Terrane is a more likely source than the Lhasa or Songpan-Ganzi terranes.

Overlap and similarity tests between the Fenghuoshan Group and all Mesozoic sedimentary units within the Tibetan Plateau are generally high but do not identify a specific sedimentary unit that may share a source terrane with the Fenghuoshan Group (Figure 9). However, when the K-S test is used to compare detrital zircon age spectra, we find that the null hypothesis is not rejected for a Lower Cretaceous sandstone collected in the Nima Basin (Figures 1, 9, and S7) [*Kapp et al.*, 2007a], indicating that the Nima Basin and Fenghuoshan Group samples may share a common source. Paleocurrent indicators for the Early Cretaceous sandstone in the Nima Basin are not reported, but paleocurrent directions from overlying Late Cretaceous volcaniclastic strata indicate southward flow [*Kapp et al.*, 2007b; *DeCelles et al.*, 2007a]. We also note that a strong detrital age peak near ~125–120 Ma is present in the detrital zircon age spectra from the Nima Basin and Fenghuoshan Group samples (Figure S7). Few of the other Mesozoic sedimentary basins analyzed for provenance have zircons of this age. Of the units compared, we consider the Nima Basin sandstone to be the one most similar to the Fenghuoshan Group based on the young zircon age peak, high values of similarity and overlap, and the results of the K-S test. Assuming paleoflow did not change in the Nima Basin between the Early and Late Cretaceous, this may suggest that the Nima Basin and Fenghuoshan Group shared a common sediment source located in the Qiangtang Terrane.

7. Discussion

7.1. Timing and Extent Deformation in Tibet Prior to the Onset of Indo-Asian Collision

The timing of nonmarine deposition within the Hoh Xil Basin places important constraints on the deformation history of the north central Tibetan Plateau by providing temporal and spatial information on the deformation of the source terrane. Controversy over the depositional age of the Fenghuoshan Group, in particular, has led to various interpretations of plateau evolution. For example, the magnetostratigraphically determined Eocene-Oligocene depositional age for the Fenghuoshan Group [*Liu et al.*, 2003] is the most prominently cited and has been used to infer the existence of an Eocene proto-plateau in central Tibet that formed shortly after the Indo-Asian collision [*C. Wang et al.*, 2008; *Dai et al.*, 2012]. However, our revised Late Cretaceous to early Eocene depositional age for the Fenghuoshan Group requires deformation of the source terrane for these strata prior to the onset of the Indo-Asian collision.

7.1.1. Central Qiangtang Terrane

Coarse sediment accumulation in the Nima Basin [*Kapp et al.*, 2007a] and in the Hoh Xil Basin likely reflects concurrent deformation and erosion of the source terrane. The presence of conglomerates within the Fenghuoshan Group suggests a proximal sediment source, which we infer to be the Tanggula Shan. We suggest that uplift and erosion of the Tanggula Shan provided sediment to the Hoh Xil and Nima Basins and that the Tanggula Shan formed a local topographic high since at least the Late Cretaceous, although whether or not the Tanggula Shan achieved modern elevation at this time is unknown.

While few studies have focused on the deformation history of the Tanggula Shan, low-temperature thermochronologic ages from the Tanggula Shan range between 65 and 39 Ma and may suggest increased cooling rates, and potentially tectonic exhumation, from Late Cretaceous to mid-Eocene time [*C. Wang et al.*, 2008; *Rohrmann et al.*, 2012]. In addition, several magmatic bodies within and proximal to the Tanggula Shan have been dated between ~70 and 40 Ma [*Roger et al.*, 2000; *Z. Duan et al.*, 2005; *Rohrmann et al.*, 2012] and overlap with the timing of sedimentation within the Hoh Xil Basin. The genesis of these magmatic bodies remains controversial. *Roger et al.* [2000] and *Q. Wang et al.* [2008] propose that southward subduction of the

Songpan-Ganzi Terrane along the Jinsha Suture generated these plutonic rocks. However, crustal thickening and uplift of the Qiangtang Terrane may have caused crustal anatexis and magmatic activity at this time [*Xu et al.*, 1985]. In either case, the ages of magmatic intrusions within the Tanggula Shan may give insight into the timing of uplift in this region. Along with concurrent sedimentation of the Hoh Xil Basin, thermochronologic data and the timing of magmatism in the central Qiangtang Terrane suggest that this region was uplifted and eroded prior to the onset of Indo-Asian collision, during Late Cretaceous to early Eocene time. Evidence for precollisional deformation, uplift, and erosion has also been reported farther south, in the Lhasa and southern Qiangtang terranes.

7.1.2. Lhasa and Southern Qiangtang Terranes

Prior to the onset of the Indo-Asian collision, the Lhasa Terrane had experienced significant crustal shortening and likely formed part of an elevated deformation belt [*Murphy et al.*, 1997; *Kapp et al.*, 2005; 2007a, 2007b; *DeCelles et al.*, 2007a; *Rohrmann et al.*, 2012]. The northernmost Lhasa Terrane, near the Banggong-Nujiang Suture, underwent deformation during Aptian to Albian time [*Kapp et al.*, 2005, 2007a]. Subsequently, deformation migrated southward to the Gangdese retroarc, where north directed contractional deformation accommodated up to 55% shortening between 105 and 53 Ma [*Kapp et al.*, 2007b]. Widespread magmatism between 69 and 50 Ma has been interpreted as slab steepening and removal of the mantle lithosphere beneath the Lhasa Terrane [*DeCelles et al.*, 2007a; *Kapp et al.*, 2007b]. Loss of the mantle lithosphere and associated rapid uplift prior to the Indo-Asian collision [*DeCelles et al.*, 2007a] is consistent with rapid erosion rates inferred by *Hetzel et al.* [2011] between 69 and 48 Ma. The cessation of large-scale shortening within the Lhasa Terrane by ~55–50 Ma, concurrent with the main phase of Linzizong magmatism [*Murphy et al.*, 1997; *Kapp et al.*, 2007b], is consistent with the establishment of low erosion rates by ~54 Ma in northern Lhasa [*Rohrmann et al.*, 2012] and may suggest the establishment of high elevation by this time.

The precollisional crustal shortening recognized in the Lhasa Terrane also extended into the southern Qiangtang Terrane and is far greater than observed Tertiary deformation [*Kapp et al.*, 2005]. The deformation history, along with the establishment of low erosion rates in the southern Qiangtang Terrane by ~45 Ma [*Rohrmann et al.*, 2012], suggests that plateau development initiated in southern Tibet before the Indo-Asian collision and may have been largely completed soon after the collision. The evidence we have presented for an elevated and eroding Tanggula Shan (central Qiangtang Terrane) by Late Cretaceous time suggests that precollisional deformation that affected the northern Lhasa and southern Qiangtang terranes also extended several hundred kilometers farther north than previously recognized. This interpretation contradicts previous suggestions for an Eocene uplift of the southern and central Tibetan Plateau due to continental collision with India [e.g., *Tapponnier et al.*, 2001; *C. Wang et al.*, 2008; *Dai et al.*, 2012].

7.2. Timing and Distribution of Syncollisional and Postcollisional Deformation and Uplift in Northern Tibet

Our provenance analysis and revised depositional age of the Fenghuoshan Group suggest that the Hoh Xil Basin was at low elevation relative to the central Qiangtang Terrane from the Late Cretaceous to earliest Eocene. However, the deformation preserved in Late Cretaceous to Oligocene strata and the high modern elevations of the Hoh Xil Basin suggest crustal shortening, thickening, and uplift of the northern Qiangtang and southern Songpan-Ganzi terranes followed Fenghuoshan Group deposition.

7.2.1. Cenozoic Deformation of Northern Tibet

In the Hoh Xil Basin, we interpret the stratigraphic relationships and radiometric ages of variably deformed volcanic units to indicate deformation between the early Eocene and late Oligocene. This is consistent with documented syndepositional deformation in the Yushu-Nangqian region to the east [*Horton et al.*, 2002; *Spurlin et al.*, 2005], regional clockwise rotation in the Xining-Lanzhou region [*Horton et al.*, 2004; *Dupont-Nivet et al.*, 2004], and the initiation of widespread deformation of the northern plateau margin soon after the onset of Indo-Asian collision [*Yin et al.*, 2008; *Clark et al.*, 2010; *Duvall et al.*, 2011].

Despite ongoing convergence between the Indian and Eurasian continents, shortening in the Hoh Xil Basin appears to have been largely complete since late Oligocene time, suggesting deformation localized elsewhere. Currently, geodetic data from across the Tibetan Plateau show localized strong gradients in geodetic velocity profiles parallel to plate convergence at its southern and northern margins in the Himalaya and Qilian Shan, respectively [*Zhang et al.*, 2004; *Allmendinger et al.*, 2007; *Gan et al.*, 2007]. This is consistent

with observed active folding and thrust faulting in those regions [*Taylor and Yin*, 2009]. Within the plateau interior, there are no reliable fault plane solutions that indicate active crustal shortening [*Molnar and Lyon-Caen*, 1989].

7.2.2. Paleoelevation of the Hoh Xil Basin

How early Cenozoic shortening in the Hoh Xil Basin relates to the attainment of high elevations across northern Tibet remains unclear. Palynological studies conducted in the Hoh Xil Basin observe a general shift from an angiosperm-dominated environment recorded in the Eocene to early Oligocene Tuotuohe Group to a gymnosperm-dominated environment, specifically with an increase in high-mountain conifers and broad-leaved drought-resistant plants and herbs, recorded in the Oligocene Yaxicuo Group [*Q. Duan et al.*, 2007; *Duan et al.*, 2008]. This faunal shift may record tectonic uplift and local elevation-related cooling from Eocene to Oligocene time. However, deep-sea isotopic data show a global decrease in temperature over this time period [*Zachos et al.*, 2001], which may be a contributing factor in the faunal shift observed in the Hoh Xil Basin.

Oxygen isotope data from lacustrine carbonates in the Fenghuoshan Group have been used to determine paleoelevations [*Cyr et al.*, 2005]. However, a range of paleoelevation values have been proposed from this data set, the variance of which results from differences in assumed dependence of $\delta^{18}O$ on elevation across northern Tibet at the time of limestone deposition [*Cyr et al.*, 2005; *DeCelles et al.*, 2007b; *Quade et al.*, 2011; *Lechler and Niemi*, 2011; *Bershaw et al.*, 2012]. Considerable variability in the dependence of $\delta^{18}O$ on elevation across northern Tibet suggests that accurate quantification of paleoelevations from oxygen isotope data is likely to be difficult [*Lechler and Niemi*, 2011; *Bershaw et al.*, 2012], which is further complicated by the likelihood that lacustrine carbonates from the Fenghuoshan Group were deposited farther south than their present location. More recent work has constrained paleoelevations from lipid biomarkers from both the Fenghuoshan and Wudaoliang Groups [*Polissar et al.*, 2009]. These data suggest that the Fenghuoshan Group carbonates used by *Cyr et al.* [2005] were extensively thermally altered and that measured oxygen isotope values may not reflect primary values. Thermal alteration of Fenghuoshan Group strata is further shown by reset apatite fission track ages reported by *C. Wang et al.* [2008], which suggest burial to temperatures in excess of 120°C, casting further doubt on the reliability of paleoelevation estimates for the Fenghuoshan Group at the time of deposition.

Despite the lack of reliable paleoelevation estimates from the Fenghuoshan Group, paleoelevation estimates of 3400–4200 m have been derived from lipid biomarkers from Wudaoliang Group lacustrine carbonate rocks [*Polissar et al.*, 2009]. Together with the lack of deformation observed in Miocene Wudaoliang strata [*Liu et al.*, 2003; *C. Wang et al.*, 2008; *Wu et al.*, 2008] and late Oligocene-aged basalt flows, these data suggest that potentially 800–1600 m of elevation gain occurred in northern Tibet since the early Miocene, but in the absence of significant surface shortening. Thus, it is debatable whether the cessation of crustal shortening within the Hoh Xil Basin signals the attainment of modern elevation. Other mechanisms for surface uplift of northern Tibet, such as lower crustal flow [*Karplus et al.*, 2011] or loss of a mantle root [*Molnar et al.*, 1993], have been proposed and could have resulted in surface uplift of 1 km or more in the absence of crustal shortening.

7.3. Tectonic Interpretation

We propose that the precollisional contractional deformation that extended from the Lhasa to the Tanggula Shan occurred during a period of relatively flat-slab subduction of the Neo-Tethyan Ocean between ~85 and 70 Ma, coincident to the onset of deposition of the Fenghuoshan Group and magmatism in the central Qiangtang Terrane. We speculate that the initial stages of slab steepening circa 70 Ma and southward expansion of the mantle wedge resulted in small-scale Late Cretaceous to early Eocene magmatism observed in the Tanggula Shan [*Roger et al.*, 2000; *Z. Duan et al.*, 2005; *Rohrmann et al.*, 2012] and may have promoted further uplift and erosion of the central Qiangtang Terrane. Thus, a wide precollisional deformation belt extended from the subduction zone north to the Tanggula Shan. As slab-steepening progressed beneath the Lhasa Terrane [*DeCelles et al.*, 2007a; *Wen et al.*, 2008], there was voluminous, widespread magmatism in southern Tibet between ~69 and 50 Ma, and the cessation of large-scale shortening and rapid erosion of the elevated margin of Eurasia [*Murphy et al.*, 1997; *DeCelles et al.*, 2007a; *Kapp et al.*, 2007b; *Rohrmann et al.*, 2012]. During the early stages of Indo-Asian collision, high gravitational potential energy inhibited further thickening and elevation gain between the collision zone and the Tanggula Shan, thus promoting the northward migration of deformation into the Hoh Xil Basin in Eocene-Oligocene time.

Our observations within the Hoh Xil Basin do not uniquely constrain the tectonic mechanisms responsible for the observed syncollisional and postcollisional sedimentation and deformation. Convergence along the Jinsha Suture could have caused flexure within the northern Qiangtang Terrane concurrent with compression localized near the suture zone, thus explaining syndeformational deposition of the Tuotuohe and Yaxicuo Groups in the Hoh Xil Basin from Eocene to late Oligocene time. Post-Early Miocene uplift in the absence of crustal shortening may have been caused by lower crustal flow [*Karplus et al.*, 2011] or the loss of a mantle root [*Molnar et al.*, 1993] beneath northern Tibet. Observed Oligocene-Miocene reactivation of the Banggong-Nujiang Suture [*Kapp et al.*, 2007a] may have been caused by the attainment of moderate to high elevations within the Hoh Xil Basin and the cessation of deformation near the Jinsha Suture. Miocene initiation of strike-slip movement along the Kunlun Fault largely follows cessation of shortening in the Hoh Xil Basin and may also indicated a major kinematic change related to high elevation within the northern plateau [*Jolivet et al.*, 2003; *Fu and Awata*, 2007; *Duvall et al.*, 2013].

8. Conclusions

Late Cretaceous shortening and elevated exhumation rates are documented within the Lhasa and southern to central Qiangtang terranes [e.g., *Murphy et al.*, 1997; *Kapp et al.*, 2007b; *DeCelles et al.*, 2007a; *Hetzel et al.*, 2011; *Rohrmann et al.*, 2012; *Dai et al.*, 2013]. However, the persistence of slow exhumation rates within the Kunlun Shan from ~ 150 Ma until 35 Ma and until ~ 40 Ma farther east suggests that Late Cretaceous deformation did not extend to the modern northern plateau margin [*Jolivet et al.*, 2001; *Clark et al.*, 2010]. The history of sedimentation and deformation within the Hoh Xil Basin provides a spatial and temporal link between the Lhasa and southern Qiangtang terranes, which deformed prior to the Indo-Asian collision, and the northern plateau margin, where thrust faults were activated in the Eocene. Thus, this region potentially records how the northern plateau responds as plate boundary forces change as the last of the Neotethys Ocean subducts and the Indian continental lithosphere collides.

In this work, we revise the depositional age range of the Fenghuoshan Group based on new biostratigraphic and radiometric age constraints and reinterpretation of published magnetostratigraphy. The thin interbedded tuff we radiometrically dated at 59.27 Ma provides a critical tie point for correlation with the geomagnetic polarity timescale. We compare detrital zircon age spectra of the Fenghuoshan Group with age spectra from Tibetan terranes and Mesozoic sedimentary sequences from across the Tibetan Plateau. Our results suggest that the Fenghuoshan Group was deposited from 85 to 51 Ma, was sourced from the Qiangtang Terrane, and may share a sediment source with Cretaceous sedimentary rocks in the Nima Basin. Based on age data and field observations, we suggest that the Tuotuohe and Yaxicuo Groups unconformably overlie Fenghuoshan Group strata. Furthermore, we interpret the Tuotuohe and Yaxicuo Groups as coeval sedimentary units during the early Oligocene. The presence of relatively undeformed Miocene lacustrine strata and ~27 Ma flat-lying volcanic rocks in the Hoh Xil Basin suggest that crustal shortening of the northern Tibetan Plateau ceased by late Oligocene time.

References

Allmendinger, R. W., R. Reilinger, and J. Loveless (2007), Strain and rotation rate from GPS in Tibet, Anatolia, and the Altiplano, *Tectonics*, *26*, TC3013, doi:10.1029/2006TC002030.

An, Y., Z. Deng, and Y. Zhuang (2004), Characteristics of the Fenghuoshan Group's material and its era discussion, *Northwestern Geol.*, *37*(1), 63–68.

Argand, E. (1924), La Tectonique de l'Asie, *Proc. Int. Geol. Congr.*, *7*, 170–372.

Bershaw, J., S. M. Penny, and C. N. Garzione (2012), Stable isotopes of modern water across the Himalaya and eastern Tibetan Plateau: Implications for estimates of paleoelevation and paleoclimate, *J. Geophys. Res.*, *117*, D02110, doi:10.1029/2011JD016132.

Boutelier, D., A. Chemenda, and J. P. Burg (2003), Subduction versus accretion of intra-oceanic volcanic arcs: Insight from thermo-mechanical analogue experiments, *Earth Planet. Sci. Lett.*, *212*(1–2), 31–45, doi:10.1016/S0012-821X(03)00239-5.

Bruguier, O., J. R. Lancelot, and J. Malavielle (1997), U-Pb dating on single detrital zircon grains from the Triassic Songpan-Ganzi flysch (central China): Provenance and tectonic correlations, *Earth Planet. Sci. Lett.*, *152*, 217–231, doi:10.1016/S0012-821X(97)00138-6.

Burg, J. P., F. Proust, P. Tapponnier, and G. M. Chen (1983), Deformation phases and tectonic evolution of the Lhasa block (southern Tibet, China), *Eclogae Geol. Helv.*, *76*(3), 643–665.

Chen, P. J. (1988), Distribution and migration of the Jehol Fauna with reference to non-marine Jurassic-Cretaceous boundary in China, *Acta Palaeontologica Sin.*, *27*, 659–683.

Chen, L., and Y. S. Xie (2011), Discussion of Paleocene-Eocene boundary of SanShui Basin, *Adv. Mater. Res.*, *236*, 2487–2490.

Clark, M. K., K. A. Farley, D. Zheng, Z. Wang, and A. R. Duvall (2010), Early Cenozoic faulting of the northern Tibetan Plateau margin from apatite (U–Th)/He ages, *Earth Planet. Sci. Lett.*, *296*(1–2), 78–88, doi:10.1016/j.epsl.2010.04.051.

Cloos, M. (1993), Lithospheric buoyancy and collisional orogenesis: Subduction of oceanic plateaus, continental margins, island arcs, spreading ridges, and seamounts, *Geol. Soc. Am. Bull.*, *105*(6), 715–737.

Condon, D., B. Schoene, S. Bowring, R. Parrish, N. Mclean, S. Noble, and Q. Crowley (2007), EARTHTIME: Isotopic tracers and optimized solutions for high-precision U-Pb ID-TIMS geochronology, *Eos Trans. AGU*, *88*(52), Fall Meet. Suppl., Abstract V41E–06.

Crane, P. R., and R. A. Stockey (1987), Betula leaves and reproductive structures from the middle Eocene of British Columbia, Canada, *Can. J. Bot.*, *65*(12), 2490–2500.

Crowley, J. L., B. Schoene, and S. A. Bowring (2007), U-Pb dating of zircon in the Bishop Tuff at the millennial scale, *Geology*, *35*, 1123–1126.

Cyr, A. J., B. S. Currie, and D. B. Rowley (2005), Geochemical evaluation of Fenghuoshan Group lacustrine carbonates, north-central Tibet: Implications for the paleoaltimetry of the Eocene Tibetan Plateau, *J. Geol.*, *113*(5), 517–533, doi:10.1086/431907.

Dai, J., X. Zhao, C. Wang, L. Zhu, Y. Li, and D. Finn (2012), The vast proto-Tibetan Plateau: New constraints from Paleogene Hoh Xil Basin, *Gondwana Res.*, *22*(2), 434–446, doi:10.1016/j.gr.2011.08.019.

Dai, J., C. Wang, J. Hourigan, Z. Li, and G. Zhuang (2013), Exhumation history of the Gangdese batholith, southern Tibetan Plateau: Evidence from apatite and zircon (U-Th)/He thermochronology, *J. Geol.*, *121*(2), 155–172, doi:10.1086/669250.

DeCelles, P. G., P. Kapp, L. Ding, and G. E. Gehrels (2007a), Late Cretaceous to middle Tertiary basin evolution in the central Tibetan Plateau: Changing environments in response to tectonic partitioning, aridification, and regional elevation gain, *Geol. Soc. Am. Bull.*, *119*(5–6), 654–680, doi:10.1130/B26074.1.

DeCelles, P. G., J. Quade, P. Kapp, M. Fan, D. L. Dettman, and L. Ding (2007b), High and dry in central Tibet during the late Oligocene, *Earth Planet. Sci. Lett.*, *253*, 389–401, doi:10.1016/j.epsl.2006.11.001.

Dewey, J. F. (1988), Extensional Collapse of Orogens, *Tectonics*, *7*(6), 1123–1139.

Dilek, Y. (2006), Collision tectonics of the Mediterranean region: Causes and consequences, *Geol. Soc. Am. Spec. Pap.*, *409*, 1–13, doi:10.1130/2006.2409(01).

Duan, Z., Y. Li, Y. Zhang, Y. Li, and M. Wang (2005), Zircon U-Pb age, continent dynamics significance and geochemical characteristics of the Mesozoic and Cenozoic granites from the Tanggula Range in the Qinghai-Tibetan Plateau, *Acta Geol. Sin.*, *79*(1), 88–97.

Duan, Q., K. X. Zhang, J. Wang, H. Yao, and J. Bu (2007), Sporopollen assemblage from the Totohe Formation and its stratigraphic significance in the Tanggula Mountains, northern Tibet, *Earth Sci.-J. China Univ. Geosci.*, *32*(5), 629–637.

Duan, Z., Y. Li, Z. Shen, X. Zhu, and C. Zhong (2007), Analysis of the evolution of the Cenozoic ecological environment and process of plateau surface uplift in the Wenquan area in the interior of the Qinghai-Tibet Plateau, *Geol. China*, *34*(4), 688–696.

Duan, Q., K. Zhang, J. Wang, H. Yao, and Z. Niu (2008), Oligocene Palynoflora, Paleovegetation and Paleoclimate in the Tanggula Mountains, northern Tibet, *Acta Micropalaeontol. Sin.*, *25*(2), 185–195.

Dupont-Nivet, G., B. K. Horton, R. F. Butler, J. Wang, J. Zhou, and G. L. Waanders (2004), Paleogene clockwise tectonic rotation of the Xining-Lanzhou region, northeastern Tibetan Plateau, *J. Geophys. Res.*, *109*, B04401, doi:10.1029/2003JB002620.

Dupont-Nivet, G., P. C. Lippert, D. J. van Hinsbergen, M. J. Meijers, and P. Kapp (2010), Palaeolatitude and age of the Indo–Asia collision: Palaeomagnetic constraints, *Geophys. J. Int.*, *182*(3), 1189–1198.

Duvall, A. R., M. K. Clark, B. A. van der Pluijm, and C. Li (2011), Direct dating of Eocene reverse faulting in northeastern Tibet using Ar-dating of fault clays and low-temperature thermochronometry, *Earth Planet. Sci. Lett.*, *304*(3–4), 520–526, doi:10.1016/j.epsl.2011.02.028.

Duvall, A. R., M. K. Clark, E. Kirby, K. A. Farley, W. H. Craddock, C. Li, and D. Y. Yuan (2013), Low-temperature thermochronometry along the Kunlun and Haiyuan Faults, NE Tibetan Plateau: Evidence for kinematic change during late-stage orogenesis, *Tectonics*, *32*, 1190–1211, doi:10.1002/tect.20072.

England, P., and D. McKenzie (1982), A thin viscous sheet model for continental deformation, *Geophys. J. Int.*, *70*(2), 295–321, doi:10.1111/j.1365-246X.1982.tb04969.x.

England, P., and M. Searle (1986), The Cretaceous-Tertiary deformation of the Lhasa block and its implications for crustal thickening in Tibet, *Tectonics*, *5*(1), 1–14.

England, P., and G. Houseman (1986), Finite strain calculations of continental deformation: 2. Comparison with the India-Asia Collision Zone, *J. Geophys. Res.*, *91*(B3), 3664–3676.

Fu, B., and Y. Awata (2007), Displacement and timing of left-lateral faulting in the Kunlun fault zone, northern Tibet, inferred from geologic and geomorphic features, *J. Asian Earth Sci.*, *29*(2–3), 253–265, doi:10.1016/j.jseaes.2006.03.004.

Gan, W., P. Zhang, Z.-K. Shen, Z. Niu, M. Wang, Y. Wan, D. Zhou, and J. Cheng (2007), Present-day crustal motion within the Tibetan Plateau inferred from GPS measurements, *J. Geophys. Res.*, *112*, B08416, doi:10.1029/2005JB004120.

Gehrels, G. E. (2000), Introduction to detrital zircon studies of Paleozoic and Triassic strata in western Nevada and northern California, *Geol. Soc. Am.*, *347*, 1–17, doi:10.1130/0-8137-2347-7.1.

Gehrels, G. P., et al. (2011), Detrital zircon geochronology of pre-Tertiary strata in the Tibetan-Himalayan orogen, *Tectonics*, *30*, TC5016, doi:10.1029/2011TC002868.

Gerstenberger, H., and G. Haase (1997), A highly effective emitter substance for mass spectrometric Pb isotope ratio determinations, *Chem. Geol.*, *136*, 309–312.

Gradstein, F. M., J. G. Ogg, M. Schmitz, and G. Ogg (2012), Geomagnetic polarity time scale, in *The Geologic Time Scale 2012 2-Volume Set*, pp. 85–113, Elsevier, B.V.

Harrison, T. M., P. Copeland, W. S. F. Kidd, and A. Yin (1992), Raising Tibet, *Science*, *255*(5052), 1663–1670.

Hetzel, R., I. Dunkl, V. Haider, M. Strobl, H. von Eynatten, L. Ding, and D. Frei (2011), Peneplain formation in southern Tibet predates the India-Asia collision and plateau uplift, *Geology*, *39*(10), 983–986, doi:10.1130/G32069.1.

Horton, B. K., A. Yin, M. S. Spurlin, J. Zhou, and J. Wang (2002), Paleocene–Eocene syncontractional sedimentation in narrow, lacustrine-dominated basins of east-central Tibet, *Geol. Soc. Am. Bull.*, *114*(7), 771–786, doi:10.1130/0016-7606(2002)114<0771.

Horton, B. K., G. Dupont-Nivet, J. Zhou, G. L. Waanders, R. F. Butler, and J. Wang (2004), Mesozoic-Cenozoic evolution of the Xining-Minhe and Dangchang basins, northeastern Tibetan Plateau: Magnetostratigraphic and biostratigraphic results, *J. Geophys. Res.*, *109*, B04402, doi:10.1029/2003JB002913.

Jaffey, A. H., K. F. Flynn, L. E. Glendenin, W. C. Bentley, and A. M. Essling (1971), Precision measurements of half-lives and specific activities of ^{235}U and ^{238}U, *Phys. Rev. C*, *4*, 1889–1906.

Ji, L. (1994), On the problem of the definition of the Fenghuoshan Group in the Tanggula Mountains area, Qinghai, *Reg. Geol. China*, *1994*(4), 373–380.

Jolivet, M., M. Brunel, D. Seward, Z. Xu, J. Yang, F. Roger, and P. Tapponnier (2001), Mesozoic and Cenozoic tectonics of the northern edge of the Tibetan plateau: Fission-track constraints, *Tectonophysics*, *343*(1–2), 111–134, doi:10.1016/S0040-1951(01)00196-2.

Jolivet, M., M. Brunel, D. Seward, Z. Xu, J. Yang, J. Malavieille, F. Roger, A. Leyreloup, N. Arnaud, and C. Wu (2003), Neogene extension and volcanism in the Kunlun fault zone, northern Tibet: New constraints on the age of the Kunlun fault, *Tectonics*, *22*(5), 1052, doi:10.1029/2002TC001428.

Kapp, P., A. Yin, T. M. Harrison, and L. Ding (2005), Cretaceous-Tertiary shortening, basin development, and volcanism in central Tibet, *Geol. Soc. Am. Bull.*, *117*(7), 865–878, doi:10.1130/B25595.1.

Kapp, P., P. G. DeCelles, G. E. Gehrels, M. Heizler, and L. Ding (2007a), Geological records of the Lhasa-Qiangtang and Indo-Asian collisions in the Nima area of central Tibet, *Geol. Soc. Am. Bull.*, *119*(7–8), 917–933, doi:10.1130/B26033.1.

Kapp, P., P. G. DeCelles, A. L. Leier, J. M. Fabijanic, S. He, A. Pullen, and G. E. Gehrels (2007b), The Gangdese retroarc thrust belt revealed, *GSA Today*, *17*(7), 4–9.

Karplus, M. S., W. Zhao, S. L. Klemperer, Z. Wu, J. Mechie, D. Shi, L. D. Brown, and C. Chen (2011), Injection of Tibetan crust beneath the south Qaidam Basin: Evidence from INDEPTH IV wide-angle seismic data, *J. Geophys. Res.*, *116*, B07301, doi:10.1029/2010JB007911.

Kidd, W. S. F., Y. Pan, C. Chang, M. P. Coward, J. F. Dewey, A. Gansser, P. Molnar, R. M. Shackleton, and S. Yiyin (1988), Geological mapping of the 1985 Chinese-British Tibetan (Xizang-Qinghai) Plateau Geotraverse route. Philosophical Transactions of the Royal Society of London. Series A, *Math. Phys. Sci.*, *327*(1594), 287–305.

Kong, X., A. Yin, and T. M. Harrison (1997), Evaluating the role of preexisting weaknesses and topographic distributions in the Indo-Asian collision by use of a thin-shell numerical model, *Geology*, *25*, 527–530, doi:10.1130/0091-7613(1997)025<0527.

Krogh, T. E. (1973), A low contamination method for hydrothermal decomposition of zircon and extraction of U and Pb for isotopic age determination, *Geochim. Cosmochim. Acta.*, *37*, 485–494.

Lechler, A. R., and N. A. Niemi (2011), Controls on the spatial variability of modern meteoric $^{\delta18}$O: Empirical constraints from the western U.S. and East Asia and implications for stable isotope studies, *Am. J. Sci.*, *311*(8), 664–700, doi:10.2475/08.2011.02.

Leeder, M. R., A. B. Smith, and J. Yin (1988), Sedimentology, palaeoecology and palaeoenvironmental evolution of the 1985 Lhasa to Golmud Geotraverse, *Phil. Trans. R. Soc. A*, *327*(1594), 107–143.

Leier, A. L., P. Kapp, G. E. Gehrels, and P. G. DeCelles (2007b), Detrital zircon geochronology of Carboniferous-Cretaceous strata in the Lhasa Terrane, southern Tibet, *Basin Res.*, *19*(3), 361–378, doi:10.1111/j.1365-2117.2007.00330.x.

Li, P., and L. Yuan (1990), The Fenghuoshan Group of palynological assemblages and their meaning, *Northwestern Geol.*, *1990*(4), 7–9.

Li, W., and Z. Liu (1994), The Cretaceous palynofloras and their bearing on stratigraphic correlation in China, *Cretaceous Res.*, *15*(3), 333–365.

Li, W., Z. Song, Z. Liou, C. Li, Z. Li, and H. Li (2005), Geologic characteristics and ore-controls of the Fenghuoshan copper ore deposit, Qinghai province, China, in *Mineral Deposit Research: Meeting the Global Challenge*, pp. 153–156, Springer, Berlin.

Li, Y., C. Wang, C. Ma, G. Xu, and X. Zhao (2011), Balanced cross-section and crustal shortening analysis in the Tanggula-Tuotuohe area, northern Tibet, *J. Earth Sci.*, *22*(1), 1–10, doi:10.1007/s12583-011-0152-2.

Li, Y., C. Wang, X. Zhao, A. Yin, and C. Ma (2012), Cenozoic thrust system, basin evolution, and uplift of the Tanggula Range in the Tuotuohe region, central Tibet, *Gondwana Res.*, *22*(2), 482–492, doi:10.1016/j.gr.2011.11.017.

Liu, Z., and C. Wang (2001a), Facies analysis and depositional systems of Cenozoic sediments in the Hoh Xil Basin, northern Tibet, *Sediment. Geol.*, *140*(3–4), 251–270, doi:10.1016/S0037-0738(00)00188-3.

Liu, Z., and C. Wang (2001b), Depositional Environment of the Tertiary Fenghuoshan Group in the Hoh Xil Basin, Northern Tibetan Plateau, *Acta Sedimentologica Sin.*, *19*(1), 28–34.

Liu, Z., C. Wang, and H. Yi (2001), Evolution and Mass Accumulation of the Cenozoic Hoh Xil Basin, Northern Tibet, *J. Sediment. Res.*, *71*(6), 971–984.

Liu, Z., X. Zhao, C. Wang, S. Liu, and H. Yi (2003), Magnetostratigraphy of Tertiary sediments from the Hoh Xil Basin: Implications for the Cenozoic tectonic history of the Tibetan Plateau, *Geophys. J. Int.*, *154*(2), 233–252, doi:10.1046/j.1365-246X.2003.01986.x.

Liu, Z., C. Wang, W. Jin, H. Yi, H. Zheng, X. Zhao, and Y. Li (2005), Oligo-Miocene depositional environment of the Tuotuohe Basin, central Tibetan Plateau, *Acta Sediment Sin.*, *23*(2), 210–216.

Manchester, S. R. (1987), The fossil history of the Juglandaceae, *Monogr. Syst. Bot. Missouri Bot. Gard.*, *21*, 1–137.

Mateer, N. J., and P. Chen (1992), A review of the nonmarine Cretaceous-Tertiary transition in China, *Cretaceous Res.*, *13*(1), 81–90.

Mattinson, J. M. (2005), Zircon U-Pb chemical abrasion (CA-TIMS) method: Combined annealing and multi-step partial dissolution analysis for improved precision and accuracy of zircon ages, *Chem. Geol.*, *220*, 47–66.

Molnar, P., and H. Lyon-Caen (1989), Fault plane solutions of earthquakes and active tectonics of the Tibetan Plateau and its margins, *Geophys. J. Int.*, *99*(1), 123–154, doi:10.1111/j.1365-246X.1989.tb02020.x.

Molnar, P., and J. Stock (2009), Slowing of India's convergence with Eurasia since 20 Ma and its implications for Tibetan mantle dynamics, *Tectonics*, *28*, TC3001, doi:10.1029/2008TC002271.

Molnar, P., P. England, and J. Martinod (1993), Mantle dynamics, uplift of the Tibetan Plateau, and the Indian Monsoon, *Rev. Geophys.*, *31*(4), 357–396.

Murphy, M. A., A. Yin, T. M. Harrison, S. B. Dürr, Z. Chen, F. J. Ryerson, W. S. F. Kidd, X. Wang, and X. Zhou (1997), Did the Indo-Asian collision alone create the Tibetan plateau?, *Geology*, *25*(8), 719–722, doi:10.1130/0091-7613(1997)025<0719:DTIACA>2.3.CO;2.

Najman, Y., et al. (2010), Timing of India-Asia collision: Geological, biostratigraphic, and palaeomagnetic constraints, *J. Geophys. Res.*, *115*, B12416, doi:10.1029/2010JB007673.

Orth, K., and J. McPhie (2003), Textures formed during emplacement and cooling of a Palaeoproterozoic, small-volume rhyolitic sill, *J. Volcanol. Geotherm. Res.*, *128*(4), 341–362.

Polissar, P. J., K. H. Freeman, D. B. Rowley, F. A. McInerney, and B. S. Currie (2009), Paleoaltimetry of the Tibetan Plateau from D/H ratios of lipid biomarkers, *Earth and Planet. Sci. Lett.*, *287*(1–2), 64–76, doi:10.1016/j.epsl.2009.07.037.

Powell, C. M. (1986), Continental underplating model for the rise of the Tibetan Plateau, *Earth Planet. Sci. Lett.*, *81*(1), 79–94.

Press, W. H., B. P. Flannery, S. A. Teukolsky, and W. T. Vetterling (1986), Numerical recipes, in *The Art of Scientific Computing*, pp. 186, Cambridge Univ. Press, Cambridge.

QBGMR (Qinhai Bureau of Geology and Mineral Resources) (1989a), Geologic map of the Tuotuohe region, scale 1:200,000.

QBGMR (Qinhai Bureau of Geology and Mineral Resources) (1989b), Geologic map of the Cuorendejia region, scale 1:200,000.

Quade, J., D. O. Breecker, M. Daeron, and J. Eiler (2011), The paleoaltimetry of Tibet: An isotopic perspective, *Am. J. Sci.*, *311*(2), 77–115, doi:10.2475/02.2011.01.

Rivera, T. A., M. Storey, M. D. Schmitz, and J. L. Crowley (2013), Age intercalibration of ^{40}Ar/^{39}Ar sanidine and chemically distinct U/Pb zircon populations from the Alder Creek Rhyolite Quaternary geochronology standard, *Chem. Geol.*, *345*, 87–98.

Roger, F., P. Tapponnier, N. Arnaud, U. Scharer, M. Brunel, Z. Xu, and J. Yang (2000), An Eocene magmatic belt across central Tibet: Mantle subduction triggered by the Indian collision?, *Terra Nova*, *12*(3), 102–108.

Rohrmann, A., P. Kapp, B. Carrapa, P. W. Reiners, J. Guynn, L. Ding, and M. Heizler (2012), Thermochronologic evidence for plateau formation in central Tibet by 45 Ma, *Geology*, *40*(2), 187–190, doi:10.1130/G32530.1.

Royden, L., and B. C. Burchfiel (1989), Are systematic variations in thrust belt style related to plate boundary processes? (the western Alps versus the Carpathians), *Tectonics*, *8*(1), 51–61.

Rowley, D. B. (1996), Age of initiation of collision between India and Asia: A review of stratigraphic data, *Earth Planet. Sci. Lett.*, *145*(1), 1–13.

Samson, S. D., and E. C. Alexander (1987), Calibration of the interlaboratory $^{40}Ar/^{39}Ar$ dating standard, MMhb-1, *Chem. Geol.*, *66*, 27–34.

Schmitz, M. D., and B. Schoene (2007), Derivation of isotope ratios, errors and error correlations for U-Pb geochronology using ^{205}Pb-^{235}U-(^{233}U)-spiked isotope dilution thermal ionization mass spectrometric data, *Geochem. Geophys. Geosyst.*, *8*, Q08006, doi:10.1029/2006GC001492.

Schoene, B., J. Guex, A. Bartolini, U. Schaltegger, and T. J. Blackburn (2010), Correlating the end-Triassic mass extinction and flood basalt volcanism at the 100 ka level, *Geology*, *38*(5), 387–390.

Şengör, A. M. C., and B. A. Natal'in (1996), Paleotectonics of Asia: Fragments of a synthesis, in *The Tectonic Evolution of Asia*, edited by A. Yin and T. M. Harrison, 486–640, Cambridge Univ. Press, New York.

Sláma, J., et al. (2008), Plešovice zircon—A new natural reference material for U–Pb and Hf isotopic microanalysis, *Chem. Geol.*, *249*, 1–35.

Smith, A. B., and J. Xu (1988), Palaeontology of the 1985 Tibet Geotraverse, Lhasa to Golmud, *Phil. Trans. R. Soc. A*, *327*(1594), 53–105.

Song, Z., and F. Huang (1997), Comparison of palynomorph assemblages from the Cretaceous/Tertiary boundary interval in western Europe, northwest Africa and southeast China, *Cretaceous Res.*, *18*(6), 865–871.

Song, Z., Y. Zheng, and J. Liu (1995), Palynological assemblages across the Cretaceous/Tertiary boundary in northern Jiangsu, eastern China, *Cretaceous Res.*, *16*(4), 465–482.

Spurlin, M. S., A. Yin, B. K. Horton, J. Zhou, and J. Wang (2005), Structural evolution of the Yushu-Nangqian region and its relationship to syncollisional igneous activity, east-central Tibet, *Geol. Soc. Am. Bull.*, *117*(9–10), 1293–1317, doi:10.1130/B25572.1.

Styron, R. H., M. Taylor, and K. Okoronkwo (2010), Database of active structures from the Indo-Asian collision, *Eos Trans. AGU*, *91*(20), 181–182, doi:10.1029/2010EO200001.

Tapponnier, P., X. Zhiqin, F. Roger, B. Meyer, N. Arnaud, G. Wittlinger, and Y. Jingsui (2001), Oblique stepwise rise and growth of the Tibet Plateau, *Science*, *294*, 1671–1677.

Taylor, M., and A. Yin (2009), Active structures of the Himalayan-Tibetan orogen and their relationships to earthquake distribution, contemporary strain field, and Cenozoic volcanism, *Geosphere*, *5*(3), 199–214.

Van Itterbeeck, J., P. Missiaen, A. Folie, V. S. Markevich, D. Van Damme, G. Dian-Yong, and T. Smith (2007), Woodland in a fluvio-lacustrine environment on the dry Mongolian Plateau during the late Paleocene: Evidence from the mammal bearing Subeng section (Inner Mongolia, PR China), *Palaeogeogr. Palaeoclimatol. Palaeoecol.*, *243*(1), 55–78.

Wang, C., X. Zhao, Z. Liu, P. C. Lippert, S. A. Graham, R. S. Coe, H. Yi, L. Zhu, S. Liu, and Y. Li (2008), Constraints on the early uplift history of the Tibetan Plateau, *Proc. Natl. Acad. Sci. U. S. A.*, *105*(13), 4987–4992, doi:10.1073/pnas.0703595105.

Wang, Q., et al. (2008), Eocene melting of subducting continental crust and early uplifting of central Tibet: Evidence from central-western Qiangtang high-K calc-alkaline andesites, dacites and rhyolites, *Earth Planet. Sci. Lett.*, *272*(1–2), 158–171, doi:10.1016/j.epsl.2008.04.034.

Weislogel, A. L., S. A. Graham, E. Z. Chang, J. L. Wooden, G. E. Gehrels, and H. Yang (2006), Detrital zircon provenance of the Late Triassic Songpan–Ganzi complex: Sedimentary record of collision of the north and south China blocks, *Geology*, *34*, 97–100, doi:10.1130/G21929.1.

Weislogel, A. L., S. A. Graham, E. Z. Chang, J. L. Wooden, and G. E. Gehrels (2010), Detrital zircon provenance from three turbidite depocenters of the Middle–Upper Triassic Songpan–Ganzi complex, central China, record of collision tectonics, erosional exhumation, and sediment production, *Geol. Soc. Am. Bull.*, *122*, 1969–1990.

Wen, D., D. Liu, S. Chung, M. Chu, J. Ji, Q. Zhang, B. Song, T. Lee, M. Yeh, and C. Lo (2008), Zircon SHRIMP U–Pb ages of the Gangdese batholith and implications for Neotethyan subduction in southern Tibet, *Chem. Geol.*, *252*(3–4), 191–201, doi:10.1016/j.chemgeo.2008.03.003.

Wu, Z., P. Ye, D. Hu, W. Zhang, and C. Zhou (2007), U-Pb isotopic dating of zircons from porphyry granite of the Fenghuoshan Mountains, northern Tibetan Plateau and its geological significance, *Geoscience*, *21*(3), 435–442.

Wu, Z., P. J. Barosh, Z. Wu, D. Hu, X. Zhao, and P. Ye (2008), Vast early Miocene lakes of the central Tibetan Plateau, *Geol. Soc. Am. Bull.*, *120*(9–10), 1326–1337, doi:10.1130/B26043.1.

Xu, R. H., U. Schärer, and C. J. Allègre (1985), Magmatism and metamorphism in the Lhasa block (Tibet): A geochronological study, *J. Geol.*, *93*(1), 41–57.

Ye, C. (1994), Succession of Cypridacea (Ostracoda) and nonmarine Cretaceous stratigraphy of China, *Cretaceous Res.*, *15*(3), 285–303.

Yi, H., X. Zhao, J. Lin, Z. Shi, B. Li, and B. Zhao (2004), Magnetostratigraphic studies of tertiary continental redbeds from the Wulanwula lake area of northern Tibetan Plateau and their geologic significance, *Acta Geoscientia Sin.*, *25*, 633–638.

Yi, H., C. Wang, Z. Shi, J. Lin, and L. Zhu (2008), Early uplift history of the Tibetan Plateau: Records from paleocurrents and paleodrainage in the Hoh Xil Basin, *Acta Geol. Sin.*, *82*(1), 206–213.

Yin, J., J. Xu, C. Liu, and H. Li (1988), The Tibetan Plateau: Regional stratigraphic context and previous work, *Phil. Trans. R. Soc. A*, *327*(1594), 5–52.

Yin, A., and T. M. Harrison (2000), Geologic Evolution of the Himalayan-Tibetan Orogen, *Annu. Rev. Earth Planet. Sci.*, *28*, 211–280.

Yin, A., Y. Q. Dang, L. C. Wang, W. M. Jiang, S. P. Zhou, X. H. Chen, G. E. Gehrels, and M. W. McRivette (2008), Cenozoic tectonic evolution of Qaidam basin and its surrounding regions (Part 1): The southern Qilian Shan-Nan Shan thrust belt and northern Qaidam Basin, *Geol. Soc. Am. Bull.*, *120*(7–8), 813–846, doi:10.1130/B26180.1.

Zachos, J., M. Pagani, L. Sloan, E. Thomas, and K. Billups (2001), Trends, rhythms, and aberrations in global climate 65 Ma to present, *Science*, *292*(5517), 686–693.

Zhao, W., and W. J. Morgan (1987), Injection of Indian crust into Tibetan lower crust: A two-dimensional finite element model study, *Tectonics*, *6*(4), 489–504.

Zhang, P. Z., et al. (2004), Continuous deformation of the Tibetan Plateau from Global Positioning System data, *Geology*, *32*(9), 809–812, doi:10.1130/G20554.1.

Zhang, Z., Z. Liu, Z. Wang, Y. Zhang, and D. Ye (2007), Ostracod Biostratigraphy of the Late Cretaceous Qingshankou Formation in the Songliao Basin, *Acta Geologica Sinica*, *81*(5), 727–737.

Zhong, X. (1989), Fenghuoshan Group geological era, Tanggula Qinghai, *Northwestern Geol.*, *1989*(6), 1–6.